MELLON INSTITUTE

NASA Research Grant NGR-39-008-014

INVESTIGATION OF STRESS CORROSION CRACKING OF TITANIUM ALLOYS

Semi-Annual Progress Report No. 2

for the Period

December 1, 1966 through May 31, 1967

By

E. G. Haney, G. Goldberg, R. E. Ernsberger, W. T. Brehm

MELLON INSTITUTE
4400 Fifth Avenue
Pittsburgh, Pennsylvania 15213

MELLON INSTITUTE

NASA Research Grant NGR-39-008-014

INVESTIGATION OF STRESS CORROSION CRACKING OF TITANIUM ALLOYS

Semi-Annual Progress Report No. 2

for the Period

December 1, 1966 through May 31, 1967

By

E. G. Haney, G. Goldberg, R. E. Ernsberger, W. T. Brehm

MELLON INSTITUTE
4400 Fifth Avenue
Pittsburgh, Pennsylvania 15213

~~Available to NASA Offices and Research Centers Only.~~

ABSTRACT

Investigations of the stress corrosion cracking of Ti-6Al-4V (foil and rod), Ti-13V-11Cr-3Al (foil) and 99^{+}%Ti (foil) in methanol-water solutions have been made. The maximum susceptibility to stress corrosion occurred at water contents varying from about 0.01 to 0.9 percent water depending first of all on the amount and kind of halogen ion present, i.e., Cl^{-}, Br^{-}, or I^{-}. Alloy and structure were found to be secondary factors. Electrode potential measurements were valuable in indicating the most susceptible solutions. The mechanism was considered to be electrochemical with corrosion proceeding along on active anodic path. The rate of crack propagation was found to correspond well for foil and rod material.

Introduction

The progress made since the Semi-Annual Progress Report No. 1 was submitted in December, 1966, is summarized in this report. Near the end of the first six-month period a start was made into investigations of titanium cracking in methanol. Preliminary results indicated that Ti-6Al-4V and Ti-13V-11Cr-3Al alloy foil failed readily in methanol solutions containing less than about one percent water. It was thought that the mechanism of cracking was associated with the onset of passivation as a function of water content.

In the second period, work has continued unabated on the mechanism of cracking in the methanol-titanium system. Some of the earlier results of these investigations were presented at the Defense Metals Information Center Seminar on "Accelerated Crack Propagation of Titanium in Methanol, Halogenated Hydrocarbons, and other Solutions" held at Battelle Memorial Institute in March.

Materials and Procedures

Two commercial titanium alloys investigated in foil form (0.002 - 0.003" thick and 1/4" wide) are part of the same material reported previously, i.e., Ti-6Al-4V and Ti-13V-11Cr-3Al. In addition, commerically pure titanium foil (0.005" thick and 1/4" wide and 3/8"

diameter Ti-6Al-4V alloy rods were investigated. The mill chemical compositions are listed in Table I and the mechanical properties are presented in Table II.

Most of the details of the material, chemicals, equipment, apparatus and testing procedures were given in Semi-Annual Progress Report No. 1. The stress corrosion tests on the foil were carried out with totally immersed samples under a dead weight load equivalent to 85 percent of yield strength unless otherwise noted. Electrode potential measurements were made on samples with no externally applied stress, and were measured with the same procedures as described previously. The potentiostatic measurements were also made as described except for the change in the method of affixing the sample to the working electrode. Previously, a square centimeter of titanium alloy foil was spot welded to the end of a piece of platinum wire and then the edges were coated with epoxy resin. Now the foil specimen is mounted on a cylindrical tapered stainless steel holder with a tapered teflon sheath. The foil specimen so mounted is under a small bending stress. The holder arrangement is free of solution leakage, can be rapidly assembled, and provides a solderless electrical contact. The holder is mounted on a Stern-Makrides assembly.[1] Data were taken starting with the cathodic side at -1 volt and proceeding to +1 volt with five minutes at a given potential setting before reading the current.

Cylindrical test pieces were machined from 3/8" rod of Ti-6Al-4V alloy. The rod was hot rolled, centerless ground and supplied

in the annealed condition. The important dimensions of the button-ended specimens were the 3" length, 1 3/8" gage length and the 0.128" - 0.136" diameter. The test specimens were chemically polished in a solution of 3 parts HNO_3 to 2 parts HF. Chemical polishing was accomplished in 15 - 25 seconds in this solution.

A polyethylene dish, 1 1/2" high with a hole bored in the center and a slit to the center hole, served as the solution holder. The sample was threaded through the center hole and a metal ring held the edges of the dish in place. Leakage through the center hole and slit was prevented by sealing with paraffin which proved resistant to methanol solutions.

The stress corrosion work for all the button-ended type specimens was done on an Instron hard-beam testing machine. A moving crosshead applied the necessary strain over a 30 second period. Then, the crosshead was locked in position. Approximately 100 milliliters of the methanol solution was added to the polyethylene dish which covered nearly the entire gage length of the specimen. Then the recording chart was switched on. The chart recorded load relaxation and time to failure of the specimen.

Experimental Results

A. Electrochemical Measurements and Time to Failure

In Figures 1 to 10 are plotted the times to failure with the corresponding electrode potential values as a function of water content in methanol with the indicated percentages of halogen salts

added. The plotted electrode potential values are those obtained after one hour in solution, e.g., see Figure II. In every case, the times to failure go through a minimum with respect to water content. Consider Figures 1, 2 and 3 which show the influence of 0.01 N solutions of HCl, NaCl, NaBr and NaI. Even though HCl drops the pH to a 0.5 value and NaCl solutions are near neutral values, nevertheless the position and depth of the respective minima are similar. NaBr and NaI displace the minimum toward lower water contents. The bottom of the minimum for NaI would appear to be at a water content below 0.01 percent. The electrode potential measurements indicate where the minimum would be expected. A horizontal portion of the curve is always observed at higher water contents which corresponds to a higher resistance to stress corrosion cracking. The minimum always occurs between 100% methanol and the break in this horizontal portion of the curve. Often the precise position of the bottom of the minimum was indicated by a change in slope, e.g., see Figures 1 and 3.

With decreasing NaCl content, the minimum moved toward higher methanol and decreased in breadth and depth, compare Figures 2, 4, 5 and 6. Several minima and maxima appeared in the time to failure curve with the 0.001 N NaCl solution and the corresponding electrode potential measurements appeared as a series of short straight lines with changing slopes or a continuous curve, Figure 5. The data points do not seem to be accurate enough to actually draw in a series of short straight lines, but it may be speculated that each change in slope indicated a minimum or maximum.

The experimental results presented thus far were all obtained from one alloy, Ti-6Al-4V, in one metallurgical condition. The beta alloy, Ti-13V-11Cr-3Al, has been tested both in the cold worked condition and after heat treatment, see Table II and Figure 7-10. The time to failure was only a matter of minutes at the bottom of the minima. Numerous minima and maxima appeared with this alloy also, see Figure 10, along with the corresponding series of short, straight lines with changing slopes for the electrode potential measurements.

Commerically pure titanium foil (99^{+}%) revealed a susceptibility to stress corrosion cracking similar to that of the alloys discussed previously whether it was cold rolled, stress relieved or fully annealed.* These metallurgical variables apparently made little difference in the time to failure, see Figures 12-14. The annealing widened the minimum somewhat and shifted the minimum toward higher water contents. Reducing the load on the specimen under exposure reduced the intensity and width of the minimum, Figures 12 and 13. Lowering the NaCl content reduced the degree of susceptibility just as was found for the Ti-6Al-4V alloy, see Figures 6 and 15. Likewise, the substitution of HCl for NaCl at the 0.01 N level gave similar times to failure, compare Figures 13 and 15.

Microscopic examination of the surface of the exposed foil revealed edge cracking and, less frequently, cracks away from any edges,

---

*Specimens of the cold rolled foil were sealed in vycor tubing under a reduced pressure of helium for heat treatment at 1025 and 1300 F. X-ray back-reflection techniques revealed some strain still in the foil as stress relieved at 1025 but 1300 F fully recrystallized the foil.

see Figures 17, 19, 21 and 22. Cracks were readily observable whether the salt added was NaCl, NaBr or NaI. Note the branching side cracks, characteristic of stress corrosion cracking and the dissolution along grain boundaries. A typical microstructure of the Ti-6Al-4V foil is present in Figure 20. Examination of the button-ended tensile specimens revealed only one instance of a crack other than the one which caused failure. This secondary crack is shown in Figure 17. The annealed 99^{+}%Ti foil always exhibited plastic deformation on the surface of the foil which clearly distinguished between the stress corrosion crack and the mechanical fracture. Figure 23 shows a crack started away from the edges of the specimen with tensile deformation on each side of the crack.

The effect of load on the time to failure for 99^{+}%Ti foil, both cold rolled and stress relieved, is shown in Figure 24. The solutions chosen were those which indicated the maximum degree of susceptibility to stress corrosion cracking at 75 percent of yield strength. There appears to be a "threshold stress" for both alloys but it should be recognized that this may merely be a shift in the position of the minimum at low stress levels.

The effect of the metal surface was investigated by chemically polishing Ti-6Al-4V foil. Approximately a quarter of the thickness was removed by the $3HNO_3$:2HF solution. A time to failure curve and electrode potential measurements were made, see Figure 25. The comparable curve for the as-received foil was taken from Figure 2.

With a different surface (polished) for the solution-metal reaction, a different time to failure curve was obtained.

Having established that electrode potential measurements were valuable aids to predicting the solutions which would give the maximum susceptibility to stress corrosion cracking, such measurements were always made first when investigating a new series of solutions. Recent studies aimed at a better understanding of the part played by the functional group of methyl compounds indicate that acetonitrile, CH_3CN, would not be susceptible at least with water contents up to ten percent, see Figure 26. Indeed, no failures have occurred in more than two months time. The comparable curve for methanol was replotted in Figure 26 from Figure 1.

The influence of cathodic and anodic polarization on the time to failure of the Ti-6Al-4V and 99^{+}%Ti foil in methanol solutions was examined. For these measurements, a platinum electrode was positioned 1/2" from the foil inside the polyethylene bottle. Current from a filtered D.C. power source was supplied through an ammeter and a variable resistor to the platinum electrode. Figures 27 and 28 summarize the results of this work. Anodic polarization decreased the time to failure while small cathodic current densities significantly increased the time to failure. This behavior is consistent with a mechanism of corrosion along an active anodic path. It is not consistent with a mechanism of hydrogen embrittlement. At the highest cathodic current densities tested, hydrogen may be involved in the two failures obtained from the Ti-6Al-4V alloy.

Cathodic and anodic polarization curves were found to be valuable for determining the change in the activity with the addition of water to methanol. The curves for Ti-6Al-4V are plotted in Figures 29 to 32 for 0.01 N solutions of HCl, NaCl, NaBr and NaI. There were no points plotted in the gap between the anodic and cathodic part of the curves where the current density readings were $\pm 1\ \mu A/cm^2$ even though data were obtained. The points were so numerous as to obstruct the graph. There was a marked difference in the rate at which the current density increased with the potential for anodic polarization. The rate was a maximum in solutions comparable to those which accelerated the stress corrosion cracking, i.e., the activity was at a maximum. With solutions containing five to ten percent water, the anodic polarization curves never attained a high current density value up to +0.8 volts, indicating a lower activity perhaps approaching passivation. When NaI was added to methanol-water solutions, even one percent water produced a high degree of passivation. Solutions saturated with NaF (less than 0.01 N) had comparatively low current density values even with only two hundredths percent water, Figure 33, substantiating that Ti-6Al-4V alloy did not seem to be susceptible to stress corrosion cracking in such solutions.

B. Crack Propagation Rates

Measurements of the rate of stress-corrosion crack propagation were taken on cylindrical specimens machined from rod as well as on specimens cut from foil. The rate studies were made with methanol

solutions selected to produce a maximum susceptibility to stress corrosion cracking, i.e., compositions corresponding to the minimum in the time to failure curve for the particular material. With the cylindrical specimens tested on the Instron testing machine, the specimens stress cracked with a minimum evident in the range from 0.02 to 0.06 percent water with 0.15 N NaCl, Figure 34.

Charts of the relaxation behavior of the cylindrical specimens showed that after the initial relaxation there was no measurable relaxation of the load until the last 10-60 minutes before fracture. Only the final relaxation portion of the charted curves was used for measuring the crack propagation rate. It was assumed that the load relaxation was directly related to the spreading of the crack if the specimens showed only a single crack. Metallography on the fractured specimens revealed no cracks, other than the one that broke the specimen, except for one isolated case. This absence of cracks indicated that the only crack was, indeed, the crack that initiated relaxation and subsequent failure of the specimen.

On examining the fracture surface, black corrosion products could easily be observed. By using a measuring eyepiece on the microscope, it was possible to determine the maximum penetration of the black corrosion products. Correlating this number, in millimeters, with the relaxation portion of the Instron curves, given in minutes, it was possible to arrive at fairly consistent rate measurements.

In Table A the solution, CH_3OH + .15 N NaCl + .03% H_2O, was held constant.

TABLE A

Crack Propagation Rates for Cylindrical Specimens in CH_3OH + .15 N NaCl + .03% H_2O Solutions at Various Stress Levels

Percentage Yield Strength	Rate (mm./hr.)
87.5	8.9
85	6.0
80	5.5
75	4.9
70	4.5

A marked dependence on the amount of stress can be noted. The crack propagation rate followed a logical order and decreased as the stress level decreased. The values ranged from 8.9 mm/hr at the highest stress level to a more reasonable 4.5 mm/hr at a stress equivalent to 70 percent of yield strength. In Table B, the stress was held constant at 85 percent of the yield strength.

TABLE B

Crack Propagation Rates for Cylindrical Specimens at 85% of Yield Strength in Solution of CH_3OH + .15 N NaCl with Variable Percentage of Water

Percentage Water	Rate (mm/hr.)
.06	5.1
.051	3.0
.04	3.9
.03	6.0
.02	3.2

The solution was CH_3OH + .15 N NaCl with the water content being the variable within the minimum of the time to failure curve. The rates varied from 3.0 mm/hr. to 6.0 mm/hr. with no observable dependence on the water content. The average rate was 4.3 mm/hr. Generally speaking, many authors have observed rates of 4 mm/hr. which would correspond quite well if one believes that stress corrosion cracking rates should be comparable in various systems.[2]

Measurments of the rate of crack propagation were made on 99^+%Ti and Ti-6Al-4V alloy foils. The foils were readily adaptable to rate measurements since no metallographic polishing was required to find the cracks. The annealed 99^+%Ti foil with its higher tensile elongation was especially adapted to crack measurements. Even when a sample failed, it was possible to measure the maximum crack. When mechanical rupturing started, the tip of the stress corrosion crack would plastically spread and distort the surrounding metal surface leaving a sharply defined edge. Figure 23 shows the edge of a fractured specimen which has developed a stress corrosion crack in the center of the specimen. The sharply defined crack is evident in the center and the distorted metal can be seen on either side.

Both the 99^+%Ti and Ti-6Al-4V foils were tested at 75 percent of the yield strength in methanol containing 0.01 N NaCl. In the 99^+%Ti system, the water content was kept at 0.65 percent corresponding to the minimum time to failure observed in Figure 13. The Ti-6Al-4V system, shown in Figure 2, required 0.3% H_2O at its apparent minimum time to failure. Specimens were loaded with the required weight and

solution but usually were removed before failure occurred. Taking the specimens off at various times and measuring the maximum crack depth in mm on the microscope yielded the crack propagation rate curves as shown in Figure 34.

The Ti-6Al-4V alloy specimens failed in shorter times than did the 99^{+}%Ti specimens but essentially showed the same crack propagation rate. A value of 3.6 mm/hr for the Ti-6Al-4V foil and a value of 4.0 mm/hr. for the 99^{+}%Ti foil was found. These values were obtained by simply measuring the slope of the straight line. Again, the incubation period was not included in the measurements. Although cracks were found other than the main crack in most specimens they were small enough to be considered negligible.

Discussion

According to the experimental evidence reported, the stress corrosion cracking of titanium in methanol-water solutions depended primarily on the solution composition, viz., the amount of water and the addition of Cl^{-}, Br^{-} or I^{-} ions. Alloying and structure appeared to be secondary factors. For instance, Ti-6Al-4V and commercially pure titanium foils exhibited a similar susceptibility to stress corrosion cracking. Also, the 99^{+}% Ti foil cracked as readily fully annealed as it did in the cold rolled condition. Such behaviour strongly implies a strictly electrochemical mechanism for the stress corrosion cracking. The effect

of cathodic and anodic polarization on specimens under load suggested a mechanism of dissolution along an active anodic path. Measured values of the rate of crack propagation were in good agreement whether the titanium contained ten percent or less than one percent of alloying elements.

The stress corrosion results which consistently show a minimum in the curves of time to failure versus water content in methanol may be explained in the following terms. The experimental evidence suggested that methanol and water alone was not sufficient to cause cracking without the presence of Cl^-, Br^-, or I^- ion. With decreasing Cl^- ion content, the minimum becomes less pronounced as shown in Figures 4, 5, 6, 14 and 15. With no added NaCl only one failure was observed, Figure 6, perhaps due to some accidental contamination because that failure could not be repeated. No other failures in the methanol-water system were observed up to 500 hours. It may be assumed that the titanium foil which is already in a passive condition before exposure would not be changed during immersion in methanol-water solutions without the halogen ions, Cl^-, Br^-, or I^-. When these halogen ions were present, the potentiostatic curves indicated that titanium became very active in solutions containing less than about one percent water, Figures 29-32. At water contents of 1 to 5 percent the curves gave evidence that added water has lowered the activity of the titanium. If it can be considered that the indicated low activity is approaching the passive condition, i.e., rates of reaction at the liquid-solid surface are very slow, then one explanation of the minimum is possible. Passivation or low activity does not occur completely at any

definite value of electrode potential or water content in methanol--rather it would occur over a range of values. Within the range of water contents where the minimum occurs, there would be active and passive areas; and as more water is added, more of the surface becomes passivated. The corrosion currents generated at the remaining active areas become progressively more intense and lead to the nucleation of a site susceptible to stress corrosion cracking.

The mechanism is similar to that described for maraging steel foils which exhibited a high susceptibility to stress corrosion cracking in aqueous solutions of 10-12 pH. It was possible to show some correspondence with the Pourbaix diagram for iron, but no such diagram exists for titanium-methanol system. The changing slopes of the electrode potential curves for the titanium alloys probably indicate changes in the surface films being formed with varying water contents in methanol.

When the metal surface becomes completely passive, no stress corrosion cracking would be expected because no corrosion sites will be available. It may be seen from Figures 2 to 10 and 12 to 16 that the times to failure generally exceed 500 hr. at the higher water contents where the specimens are considered to be nearly passivated. The shift in the percentage water at which the minimum occurs for the different salts and salt contents merely illustrates the varying water content at which passivation could be completed.

Conclusions

The following conclusions are based on the work accomplished in the period of December, 1966 through May, 1967.

1. The high susceptibility to stress corrosion cracking of Ti-6Al-4V (foil and rod) 99^{+}% Ti (foil) and Ti-13V-11Cr-3Al foil in chloride-, bromide-, or iodide-containing methanol solutions with up to about one percent water was attributed to electrochemical factors. Corrosion along an active anodic path involving the Cl^{-}, Br^{-}, or I^{-} ion was concluded to be the mechanism of cracking in methanol-water solutions.

2. Susceptibility to stress corrosion cracking increased markedly with NaCl content of the solution; the range of water contents over which passivation occurred was reduced with a wider range of high susceptibility resulting and a decreasing time for specimen failures. The minimum in the time-to-failure as a function of water content in methanol was shifted towards higher percentage water.

3. Measurements of electrode potential predicted the necessary water content at which maximum stress corrosion susceptibility would occur. The exact water content depended primarily on the amount and kind of halogen ions present and secondarily on such factors as alloying elements in titanium, heat treatment, and surface condition.

4. Values of the rate of crack propagation obtained from measurements on foil and rod of Ti-6Al-4 V alloy and on 99^{+}% Ti foil were similar, 3.6, 4.3, and 4.0 mm/hr. respectively. These rates are comparable with those found by other investigators for other systems.

Future Work

The following idems of work are planned for the immediate future.

1. Continued studies are planned of the correlation of electrochemical measurements with stress corrosion susceptibility in alcohol solutions on three alloys in foil form, namely, Ti-5Al-5Sn-5Zr, Ti-8Al-1Mo-1V and Ti-6Al-2Sn-4Zr-2Mo.
2. The effect of impurities in the methanol, such as acetone and formaldehyde, will be explored.
3. Additional work with specimens machined from rod is planned for a hard-beam tensile machine.

References

(1) M. Stern and A. C. Makrides, "Electrode Assembly for Electrochemical Measurements," J. Electrochem. Soc., 107, 1960, p. 782.

(2) R. N. Parkins, "Stress-Corrosion Cracking," Metallurgical Reviews, Vol. 9, No. 35, 1964, p. 250.

(3) J. A. S. Green and E. G. Haney, "Relationships between Electrochemical Measurements and Stress Corrosion Cracking of Maraging Steel," Corrosion, 23, January, 1967, p. 5.

Table I

Chemical Composition, Weight Percent

Alloy	C	O	V	Al	H	N	Fe	Cr
6Al-4V (foil)	.02	.134	4.0	6.0	.001	.01	.21	--
6Al-4V (rod)	.02	.102	4.2	6.3	.006	.007	.24	--
13V-11Cr-3Al (foil)	.016	--	13*	3*	.007	.017	.08	11*
Titanium (99^{+}) foil	.025	.38 max.	--	--	.005	.016	.14	--

*Nominal

Table II

Mechanical Properties of Titanium Alloys

Alloy	Treatment	Tensile Strength, KSI	Yield Strength KSI, 0.2% off set	Elongation, percent in 4 in.
13V-11Cr-3Al (foil)	Cold rolled	181.6	172.8	3.75
13V-11Cr-3Al (foil)	Slow heat to 1400°F, held 10 min. and C.W.Q. + 24 hr. at 900°F	175.2	165.6	4.88
6Al-4V (rod)	Hot rolled and annealed	144.0	143.5	8.2 (in 1.25 in.)
6Al-4V (foil)	Cold rolled and annealed	170.5	131.7	12.8
Titanium (99^{+}) foil	Cold rolled	137.8	124.5	6.2
Titanium (99^{+}) foil	Annealed 2 hr. at 1025°F*	90.0	80.8	21.5
Titanium (99^{+}) foil	Annealed 2 hr. at 1300°F †	100.4	81.6	28

*Some strain revealed by X-ray back-reflection techniques
†Completely recrystallized

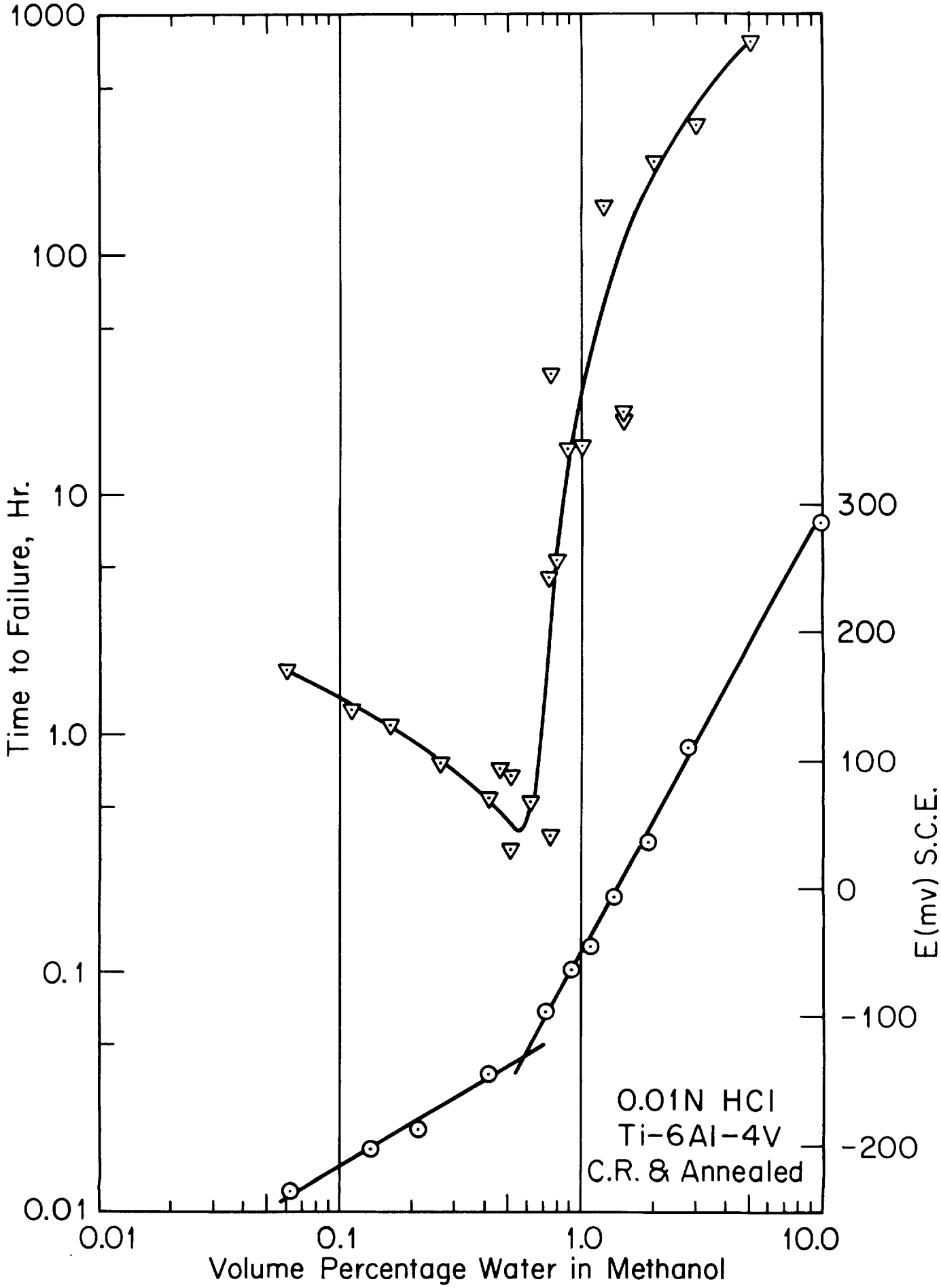

Figure 1 Comparison of time to failure with one-hour electrode potential value.

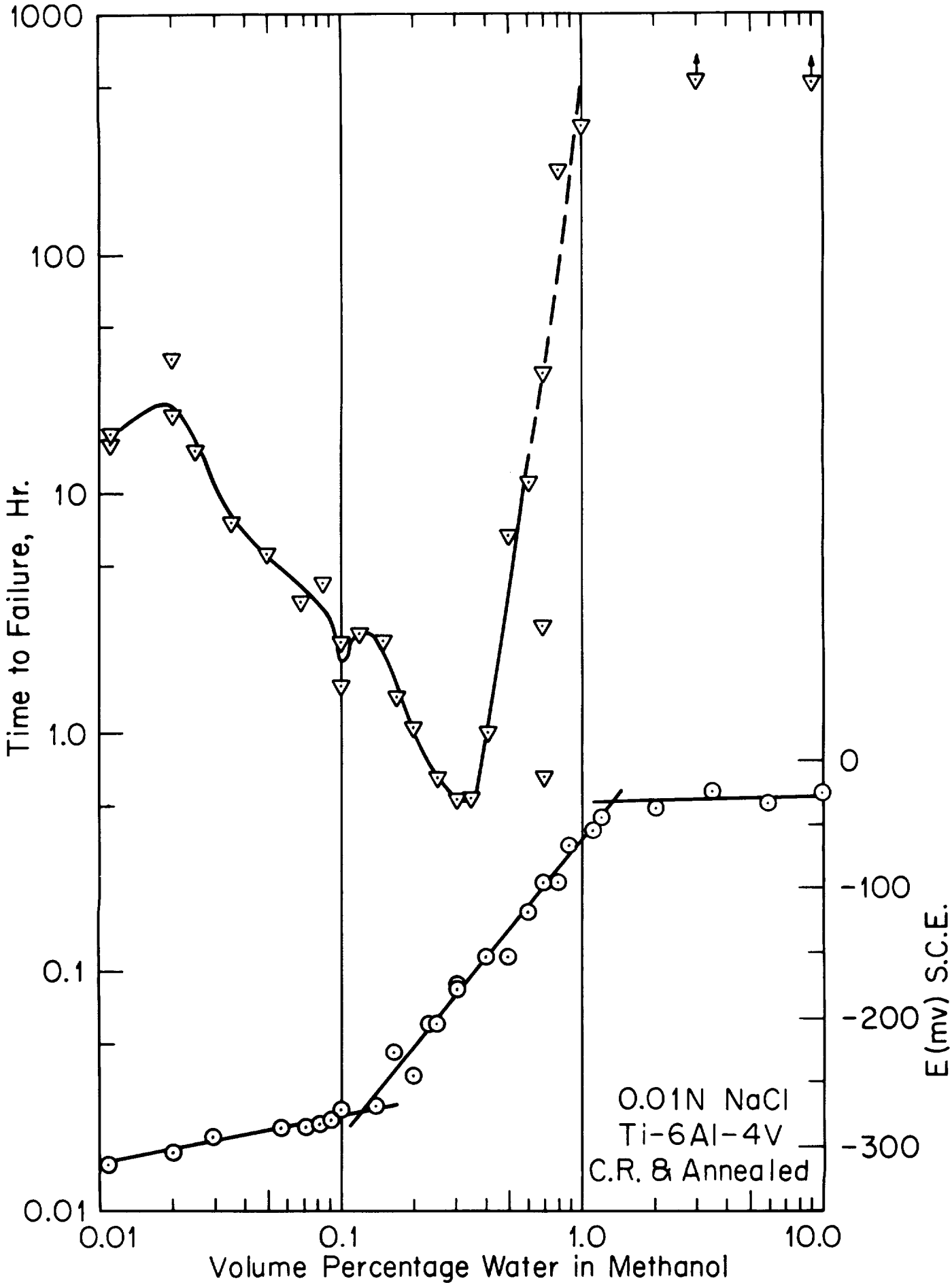

Figure 2 Comparison of time to failure with one-hour electrode potential value.

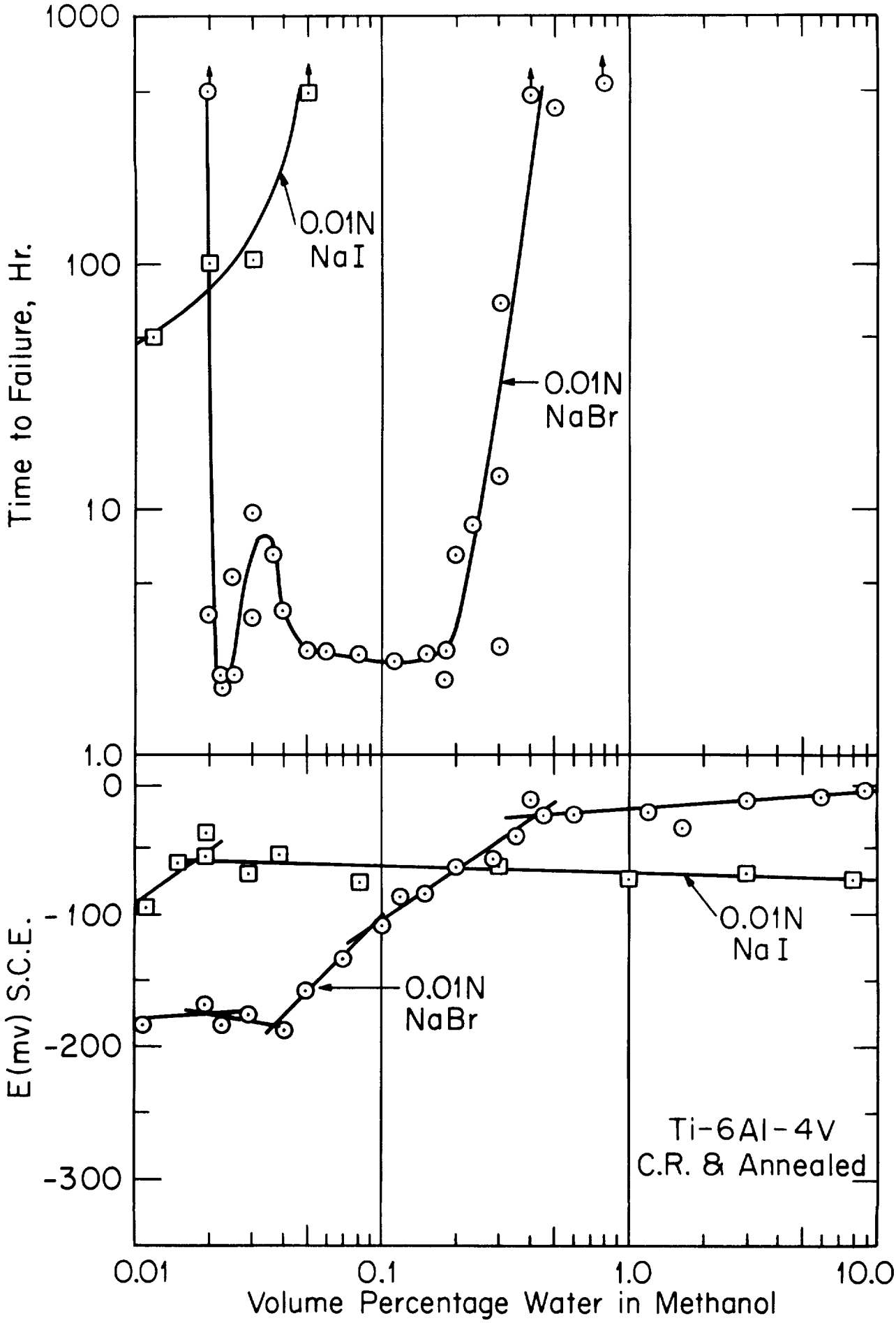

Figure 3 Comparison of time to failure with one-hour electrode potential value.

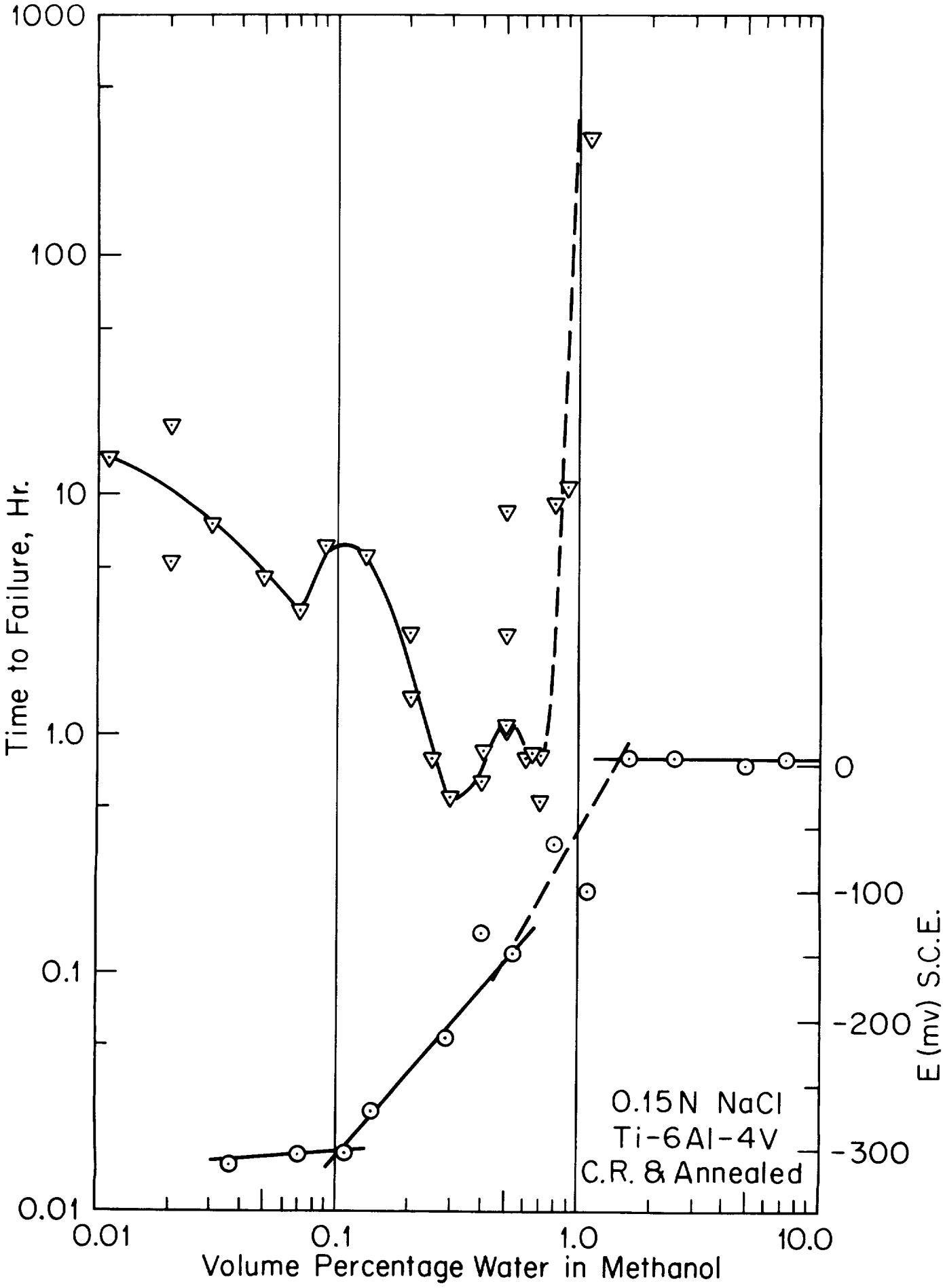

Figure 4 Comparison of time to failure with one-hour electrode potential value.

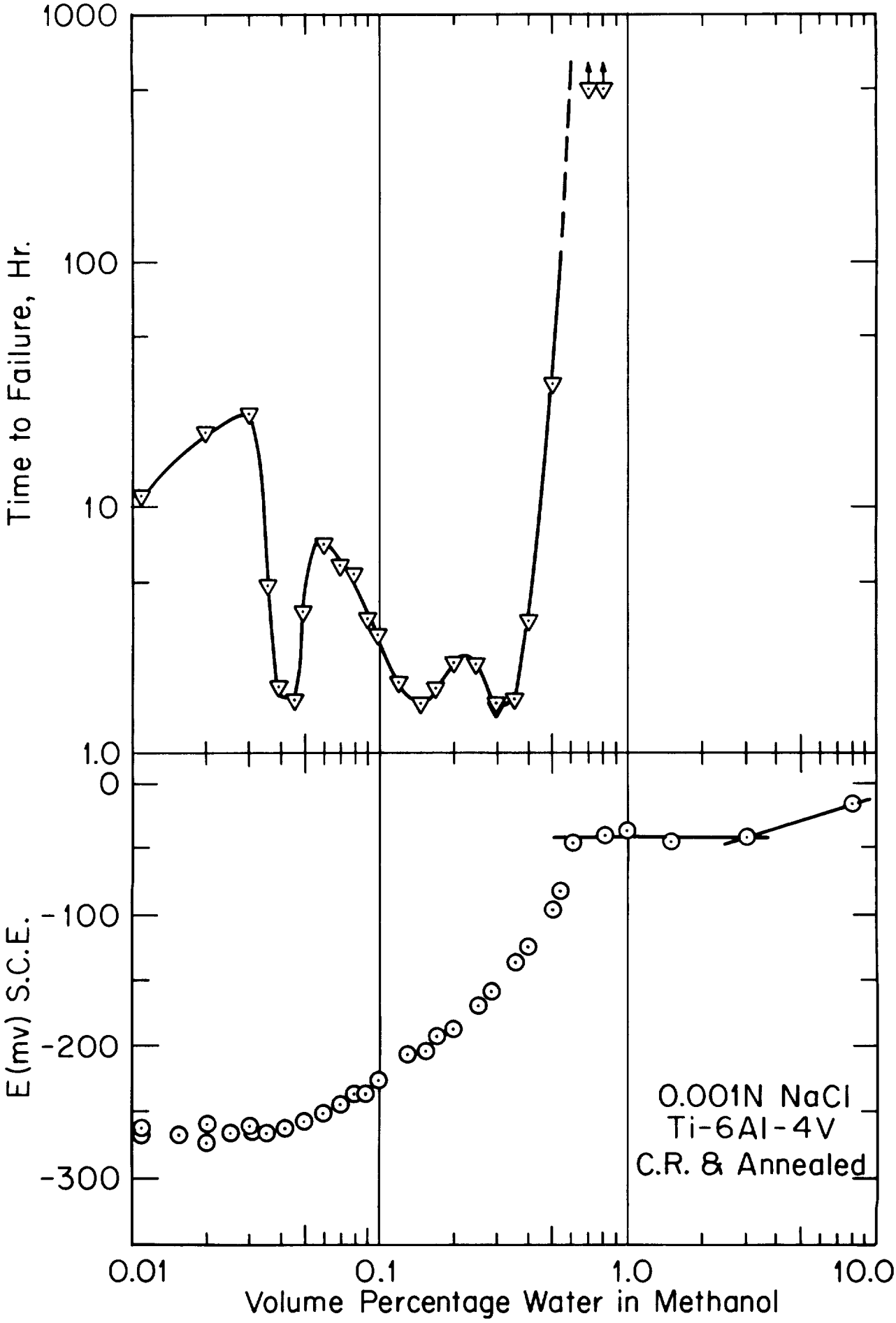

Figure 5 Comparison of time to failure with one-hour electrode potential value.

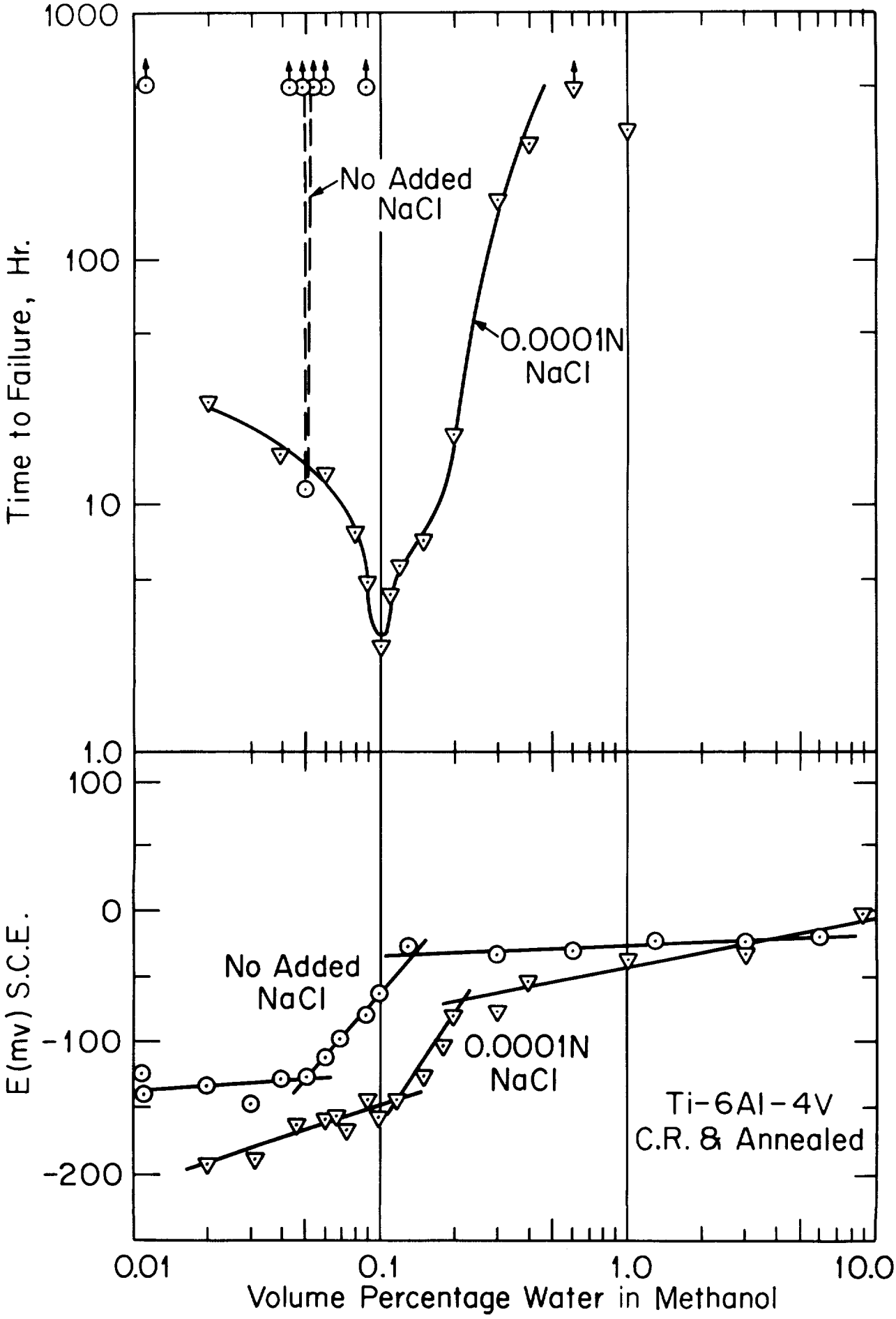

Figure 6 Comparison of time to failure with one-hour electrode potential value.

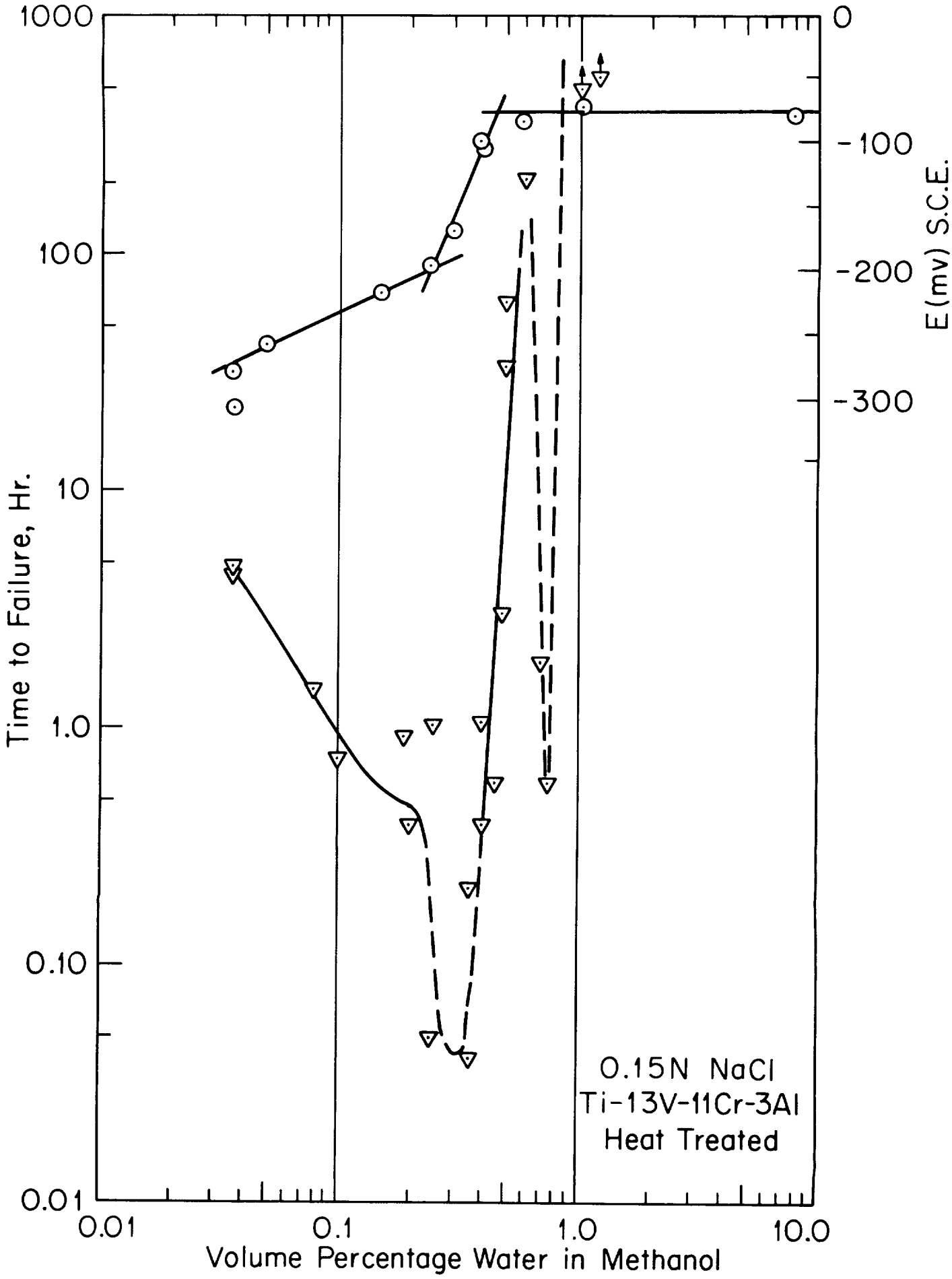

Figure 7 Comparison of time to failure with one-hour electrode potential value.

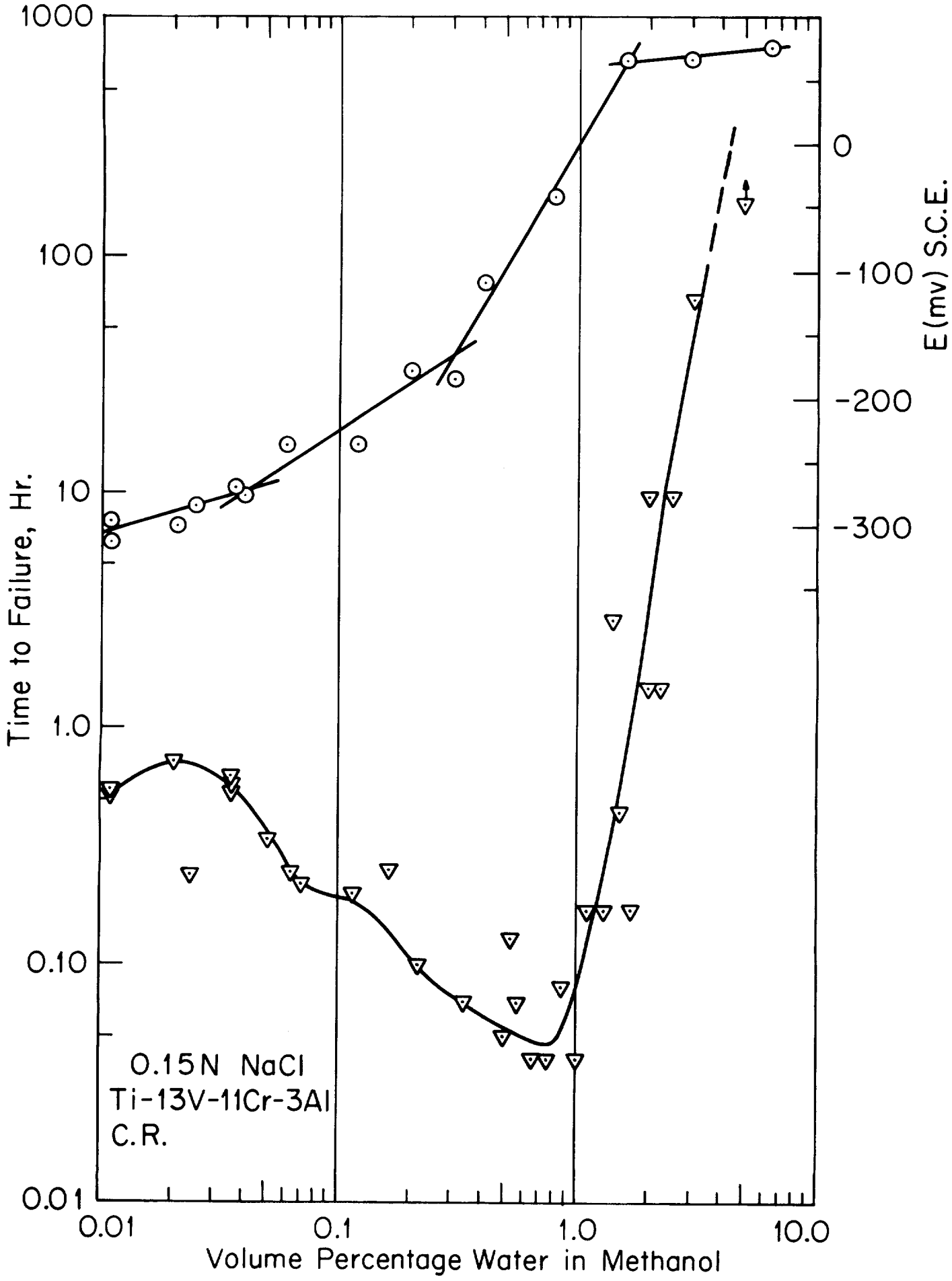

Figure 8 Comparison of time to failure with one-hour electrode potential value.

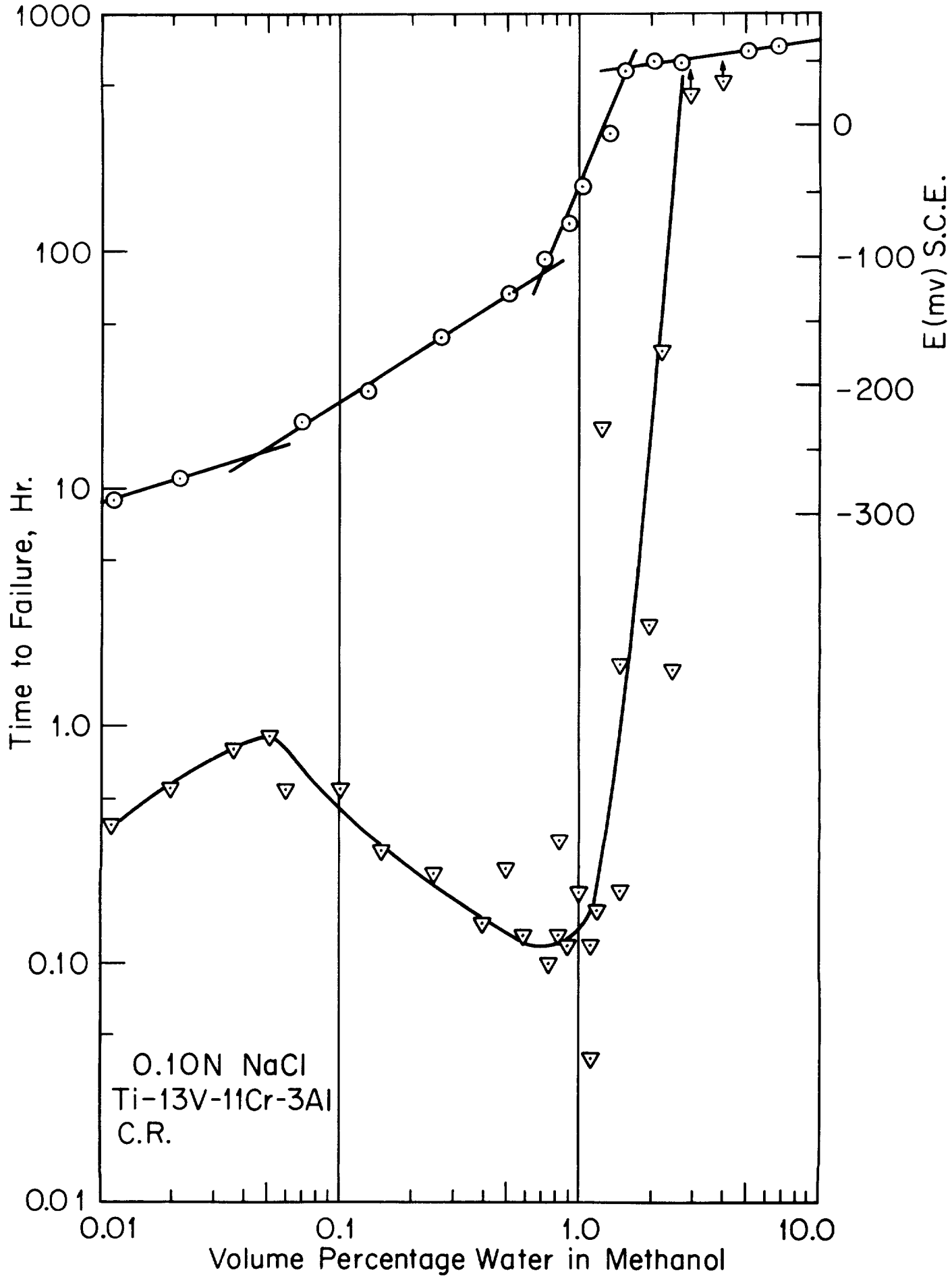

Figure 9 Comparison of time to failure with one-hour electrode potential value.

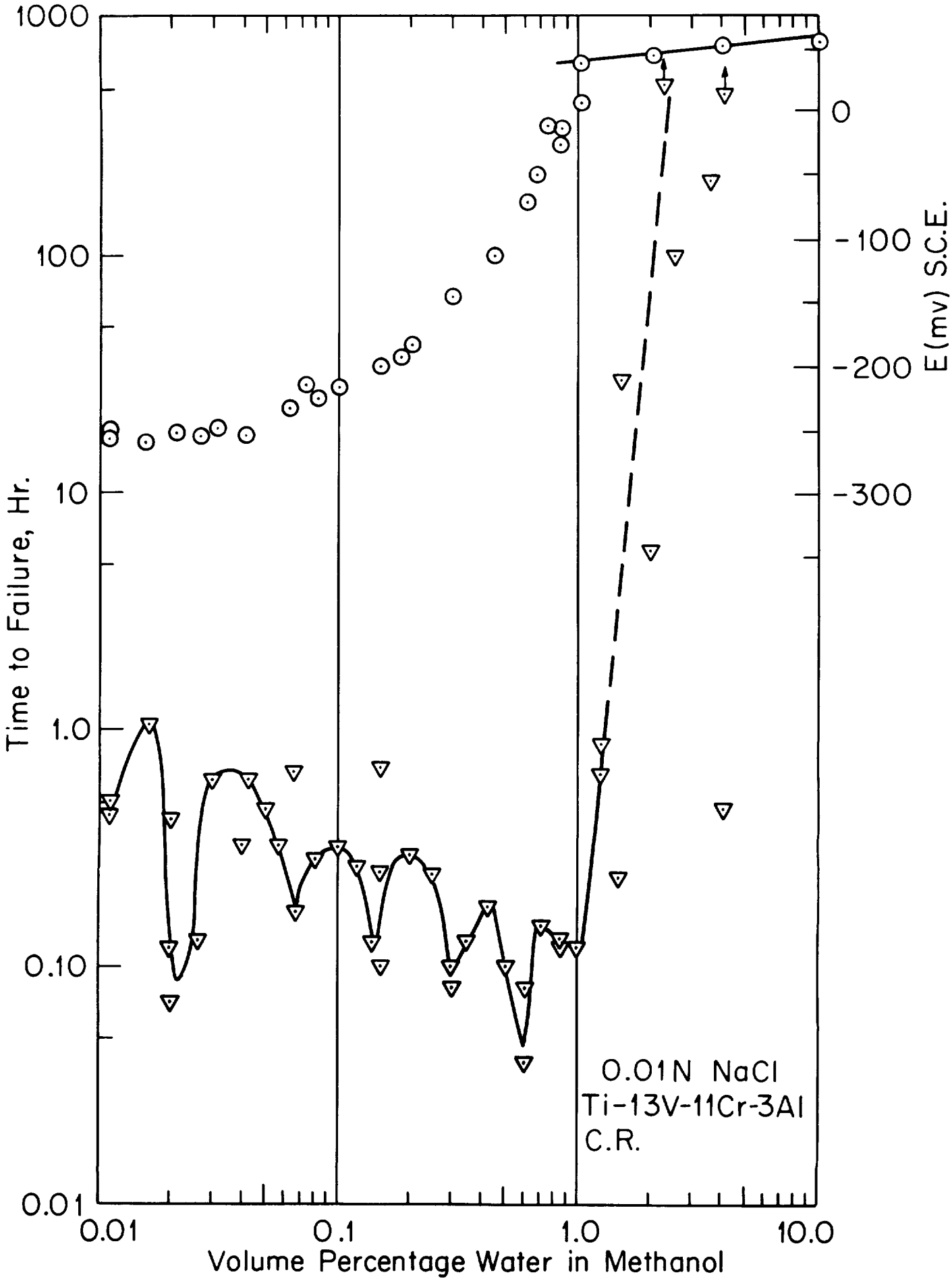

Figure 10 Comparison of time to failure with one-hour electrode potential value.

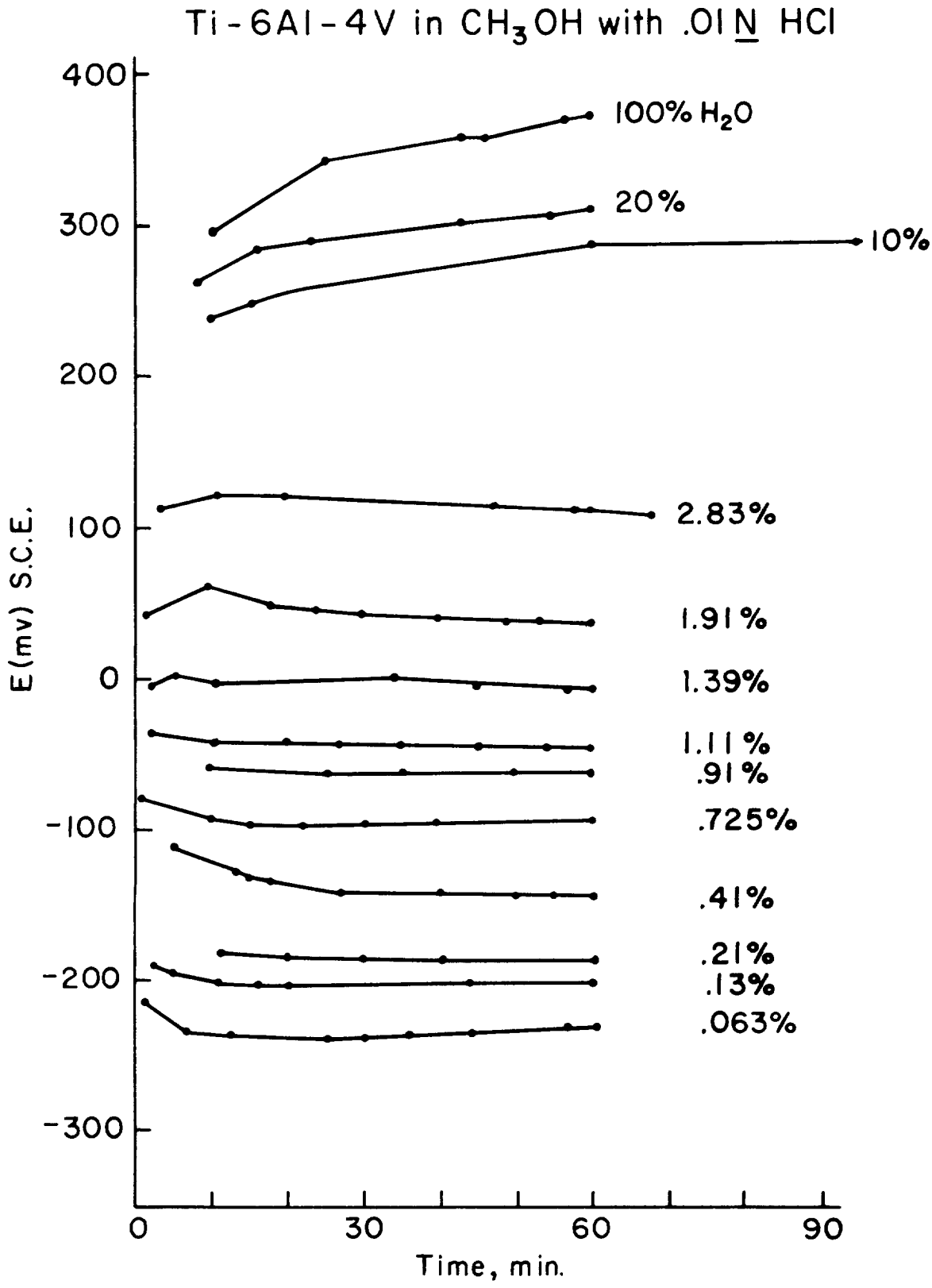

Figure 11 Electrode potential measurements as a function of time and water content.

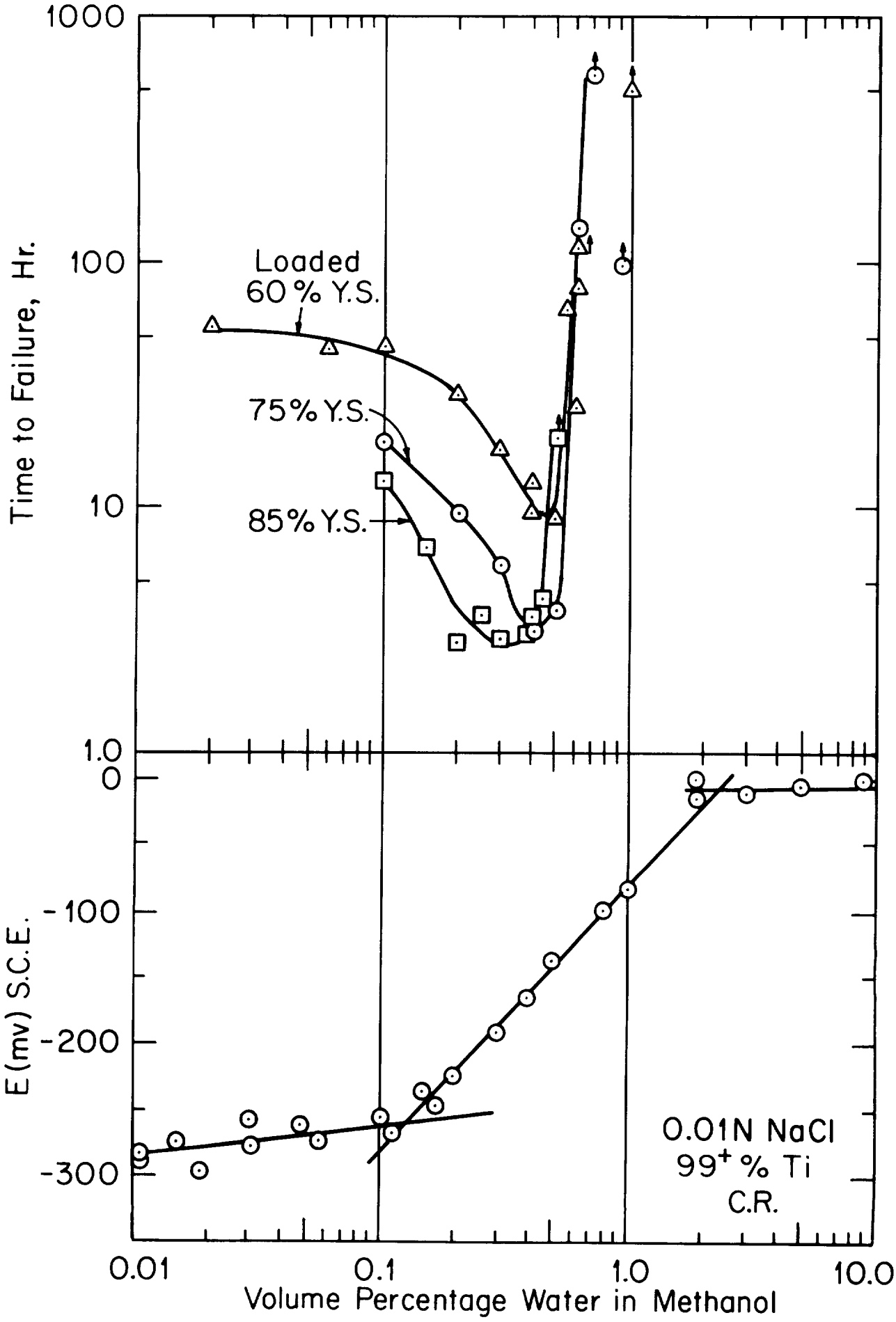

Figure 12 Comparison of time to failure at various stress levels with one-hour electrode potential value.

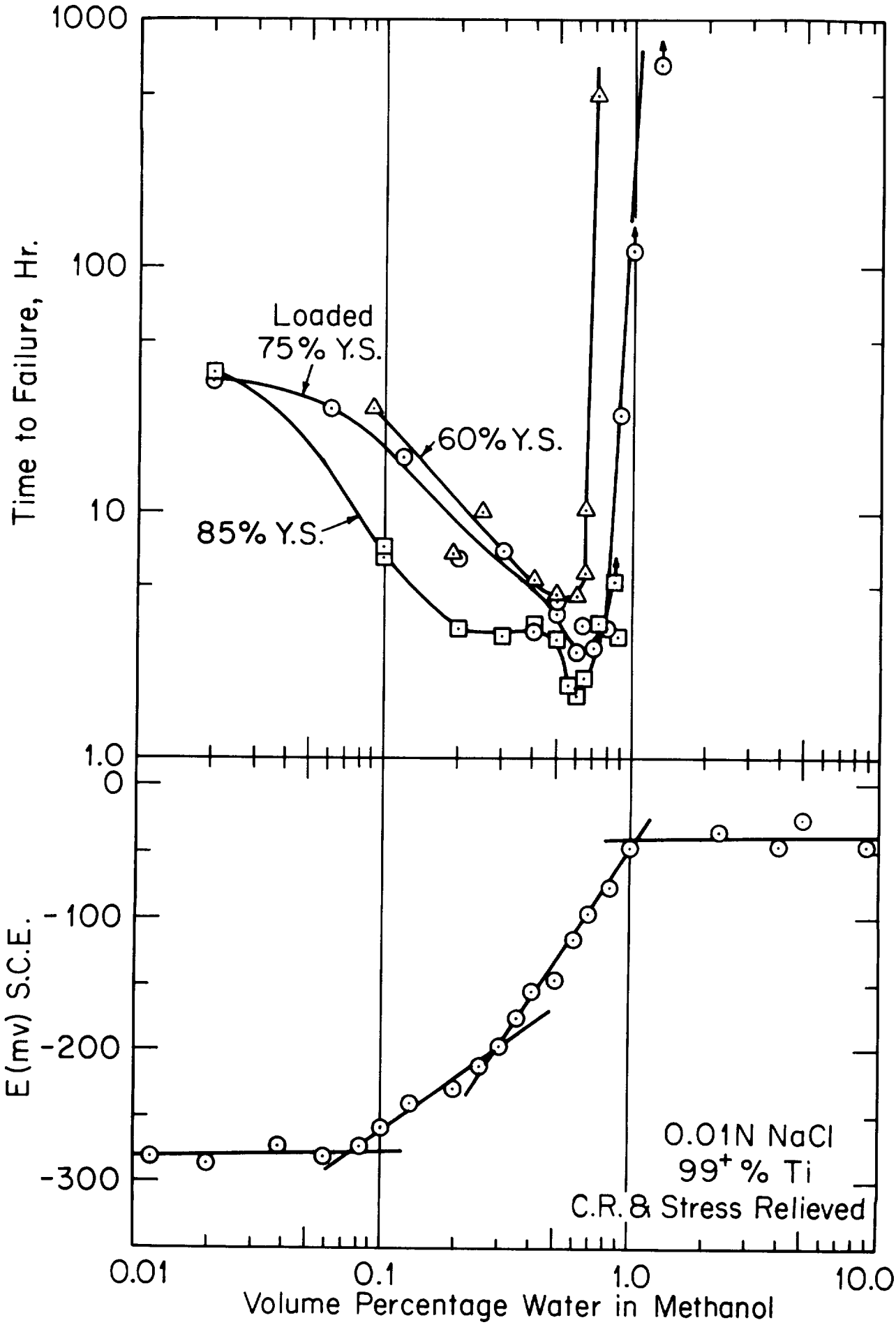

Figure 13 Comparison of time to failure at various stress levels with one-hour electrode potential value.

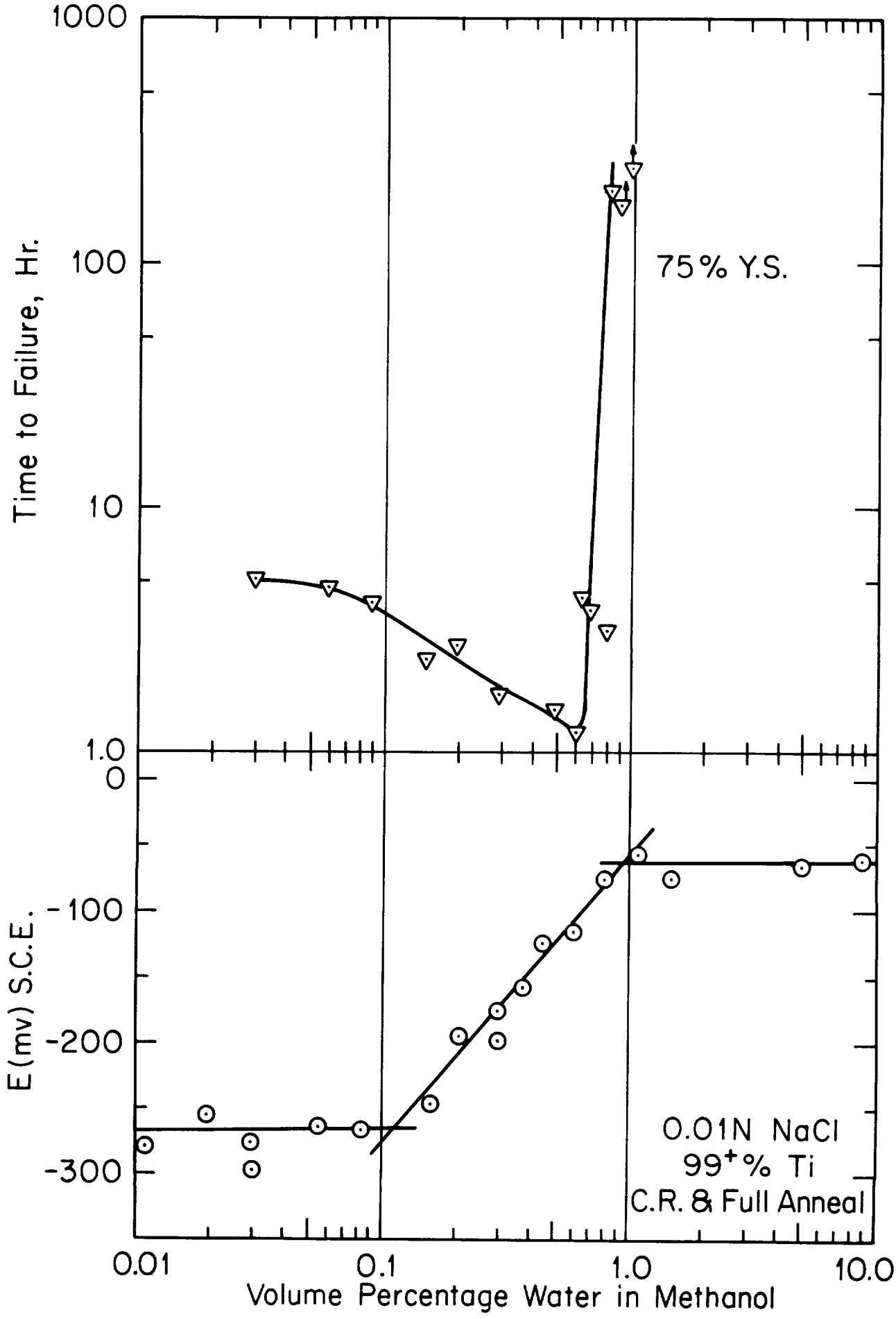

Figure 14 Comparison of time to failure with one-hour electrode potential value.

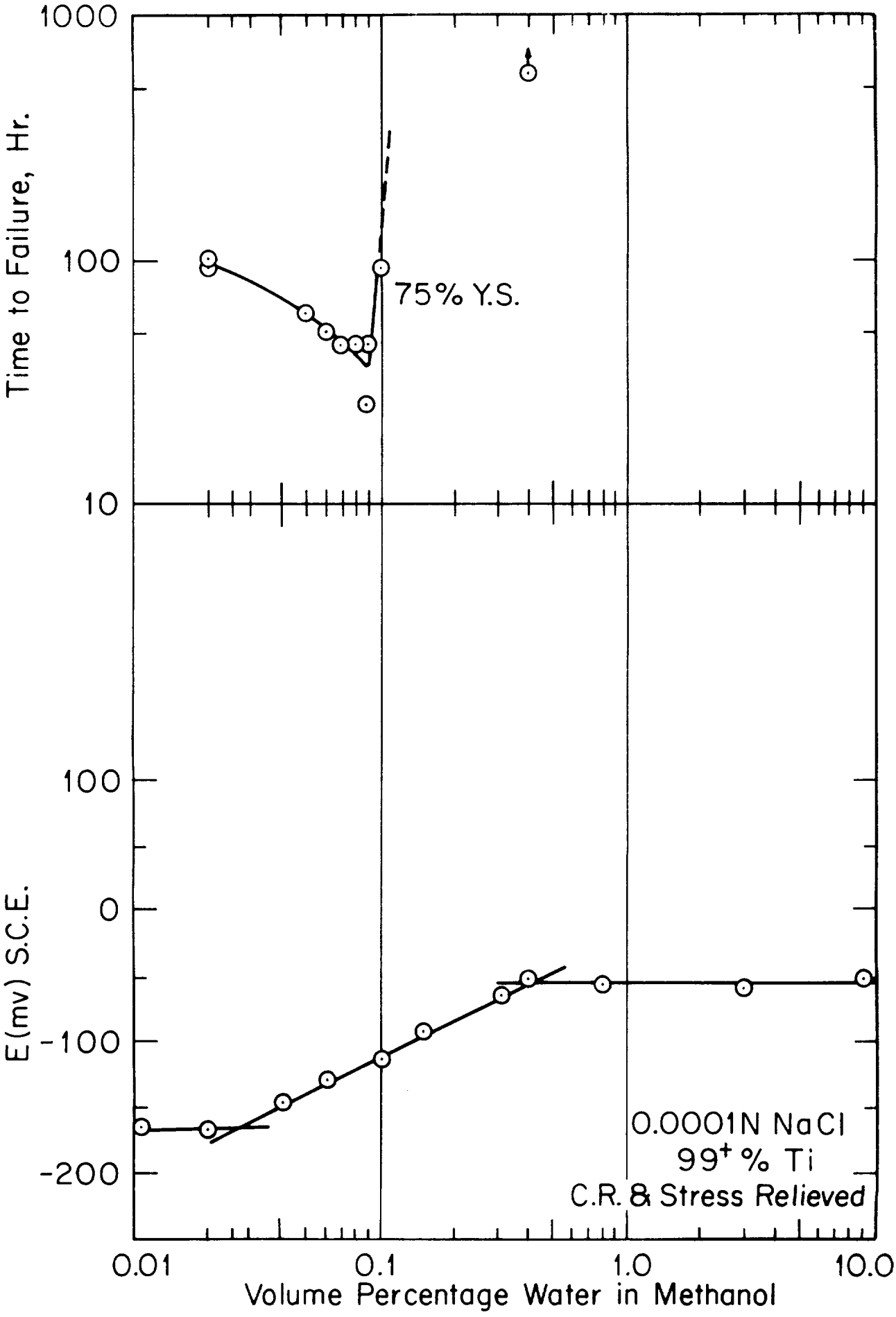

Figure 15 Comparison of time to failure with one-hour electrode potential value.

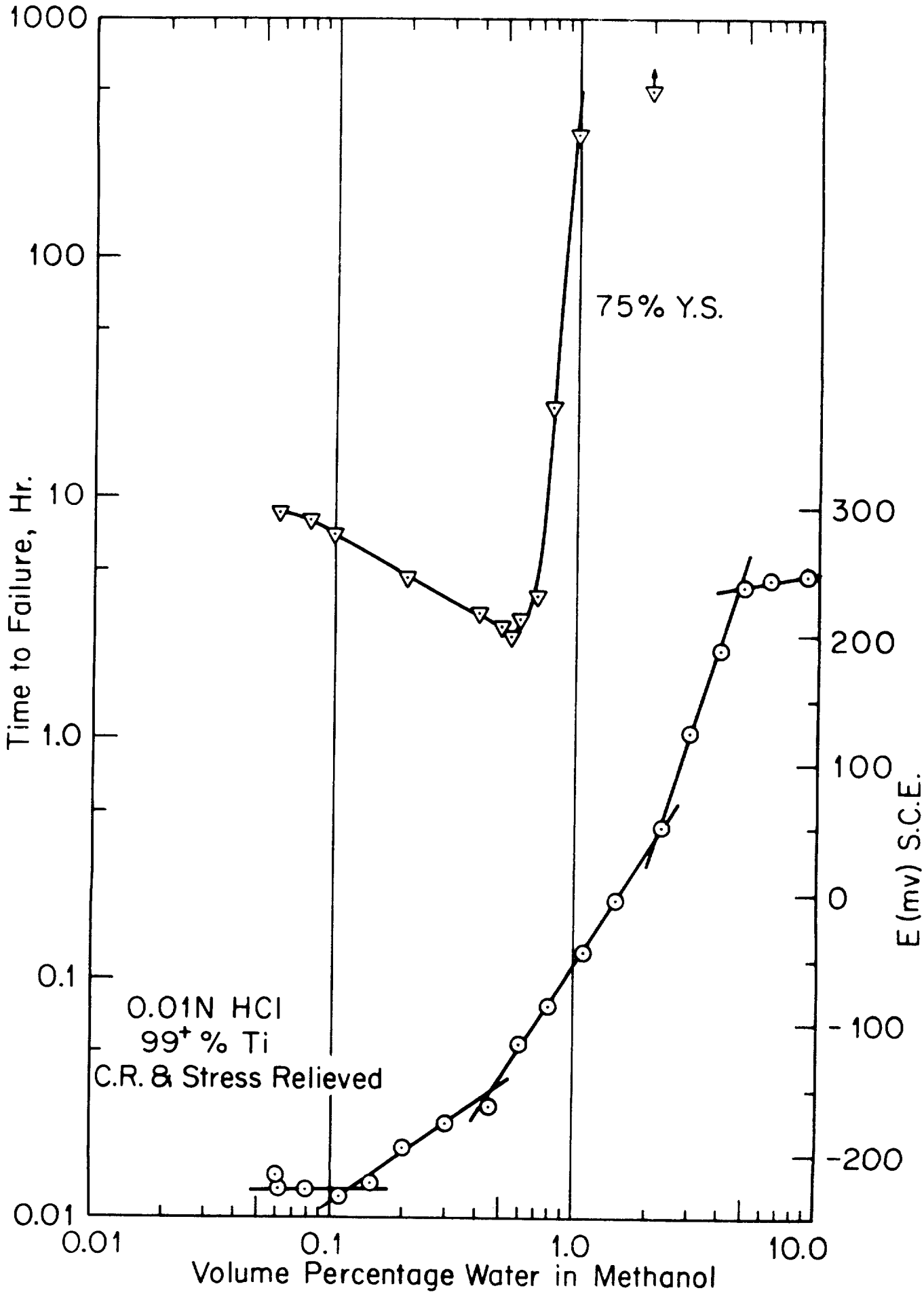

Figure 16 Comparison of time to failure with one-hour electrode potential value.

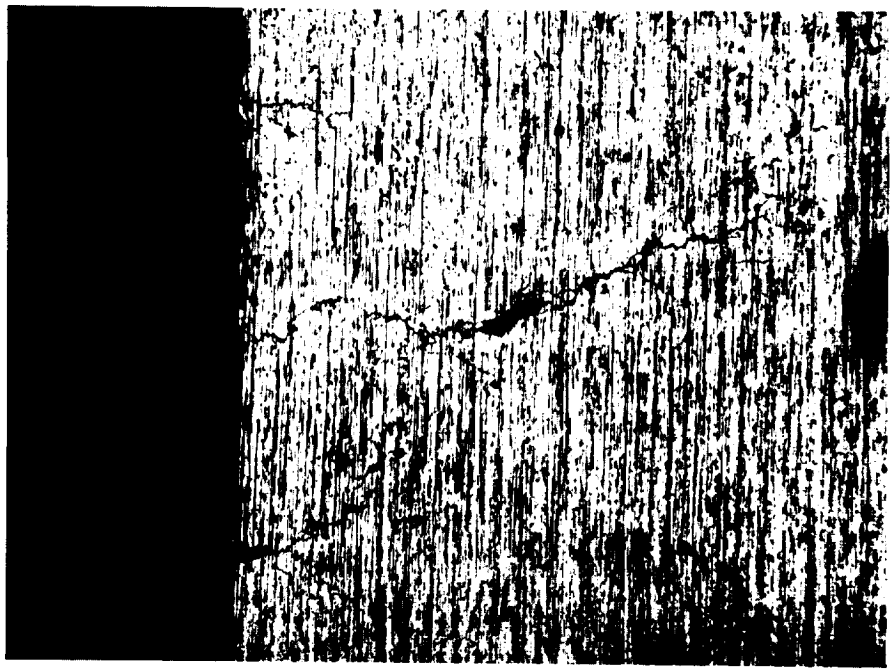

Figure 17 - Photomicrograph of the surface of 99^{+}% Ti foil, cold rolled and stress relieved, showing stress corrosion cracks developed near the edge of the specimen during immersion in CH_3OH containing 0.01 N NaCl and 0.8% H_2O; stressed 75% X 5; Mag. 63 X.

Figure 18 - Stress corrosion crack in Ti-6Al-4V alloy rod immersed in CH_3OH containing 0.15 N NaCl and 0.03% H_2O; stressed 70% Y.S., Mag. 63 X.

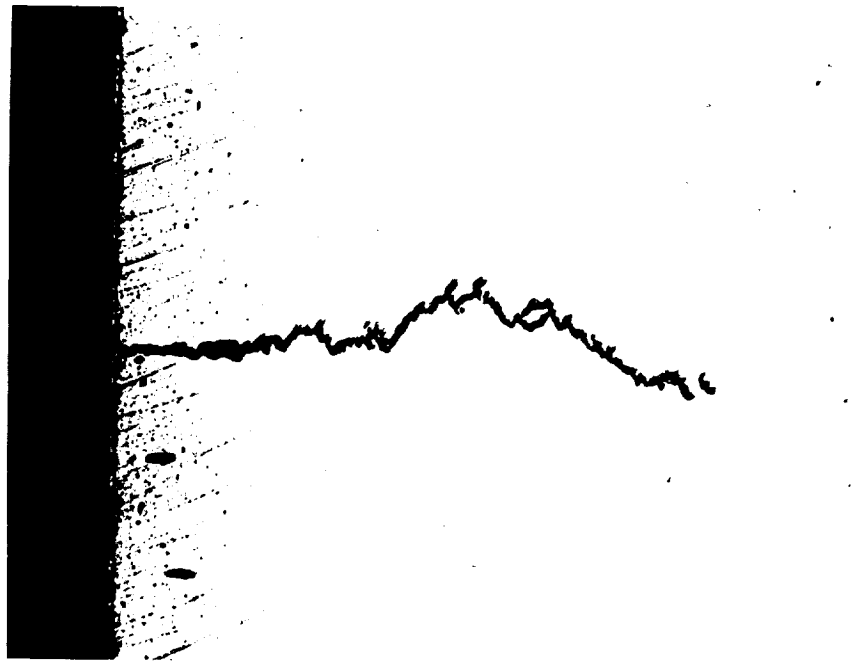

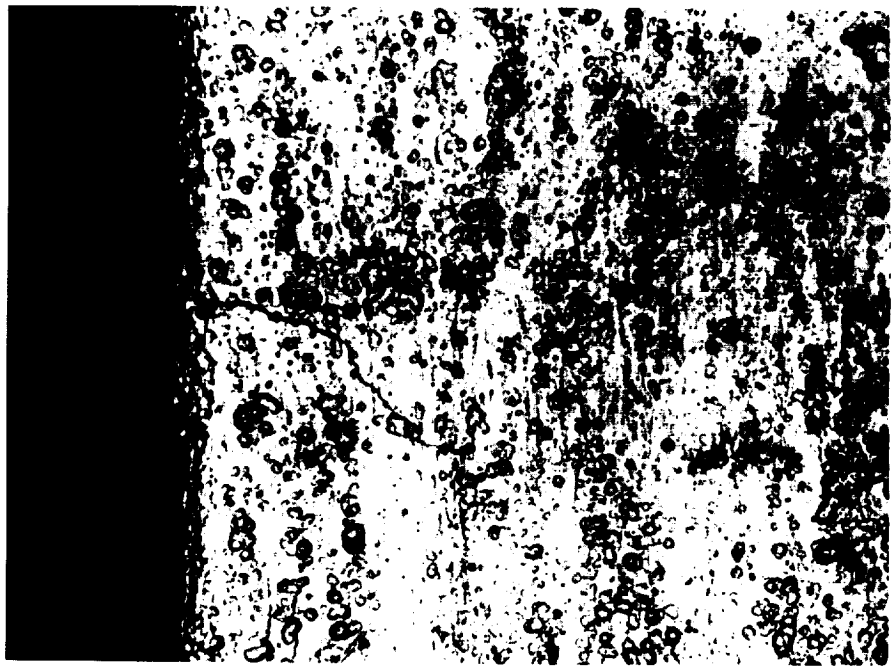

'hotomicrographs of Ti-6A1-4V alloy foil, cold rolled and annealed.

'igure 19--Cracks developed during immersion in CH_3OH containing 0.01N NaI and 0.04% H_2O; stressed 85% Y.S., Mag. 260 X.

'igure 20--Microstructure through the thickness parallel with the roll direction; etch: $3HNO_3$ + 2HF + $95H_2O$, Mag. 935 X.

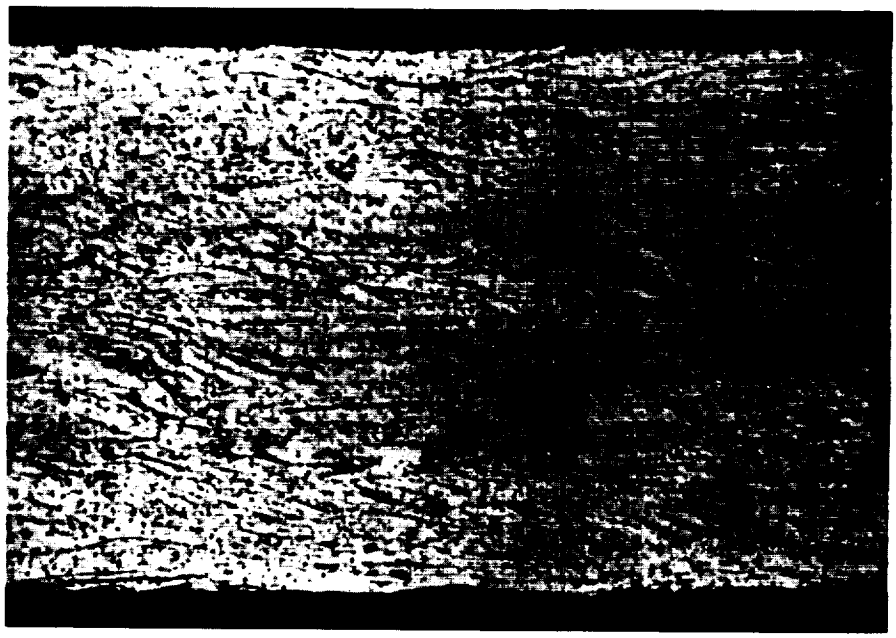

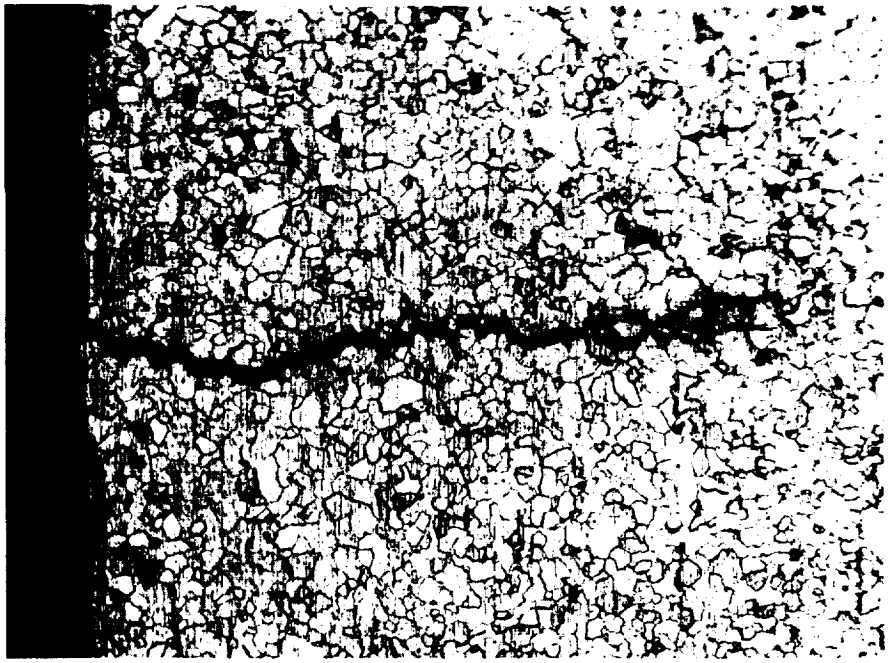

Photomicrographs of the etched surface of 99^{+}% Ti foil, cold rolled and fully annealed, showing the progression of the stress corrosion cracks along the grain boundaries and the dissolution along the crack. Cracks developed during exposure to CH_3OH containing 0.01 N NaCl and 0.7% H_2O; stressed 75% Y.S.; etch: 3 parts HNO_3 + 2 HF + 95% H_2O.

Figure 21--A crack near the fracture, Mag. 100 X.

Figure 22 - Another crack in same specimen, Mag. 250 X.

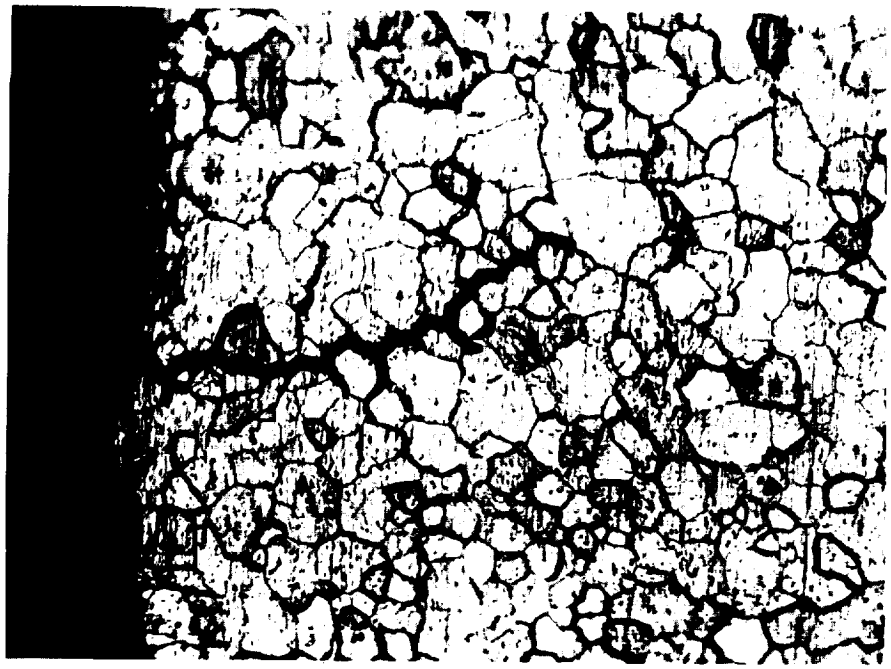

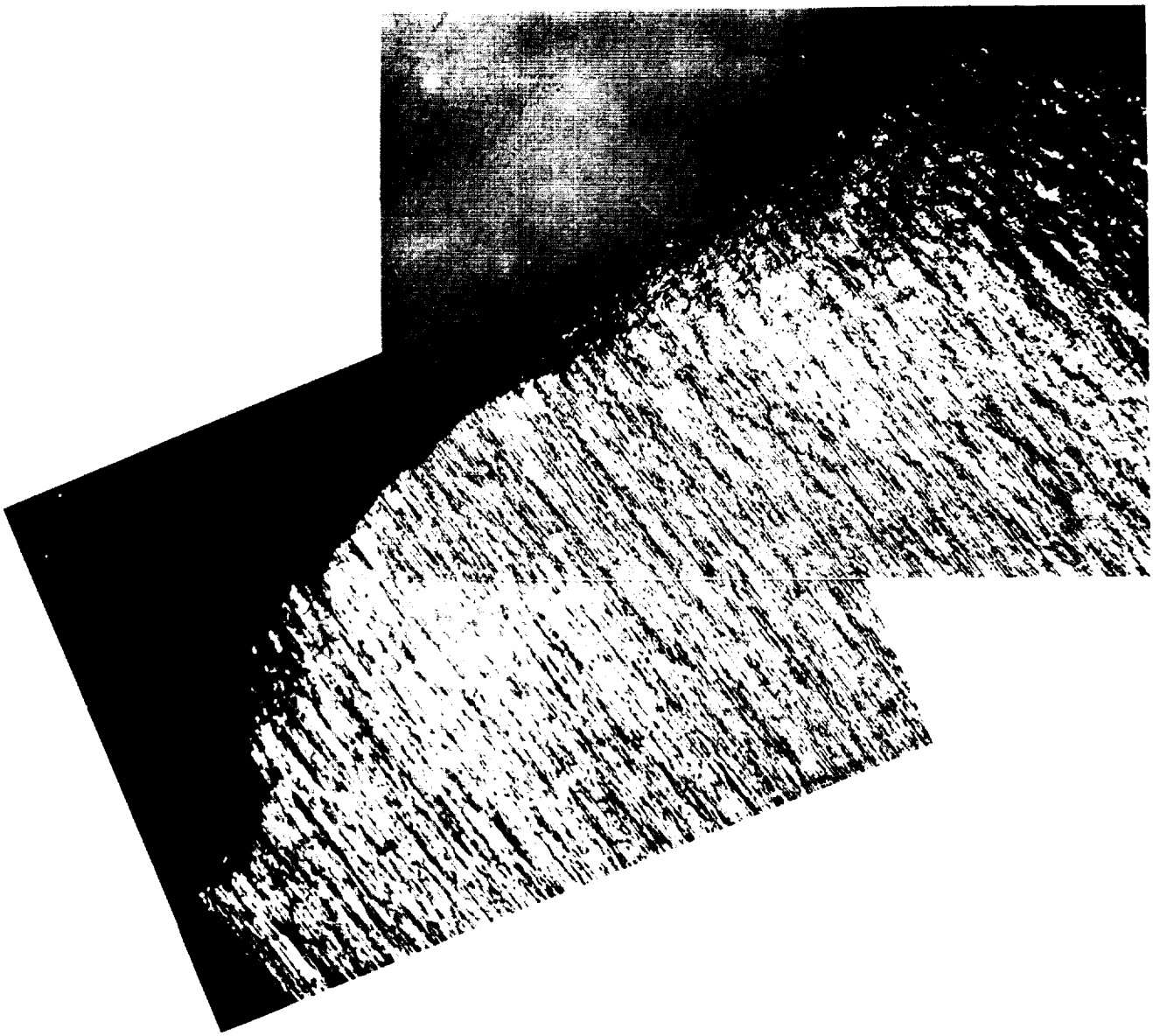

Figure 23 - The full width of a fractured 99^{+}% Ti foil, cold rolled and stress relieved, is shown. Specimen developed a crack in the center of the foil during exposure to CH_3OH containing 0.01 N NaCl and 0.65% H_2O. Plastic deformation is evident from the edge of the crack to both specimen edges. Specimen stressed 75% Y.S.; Mag. 30 X.

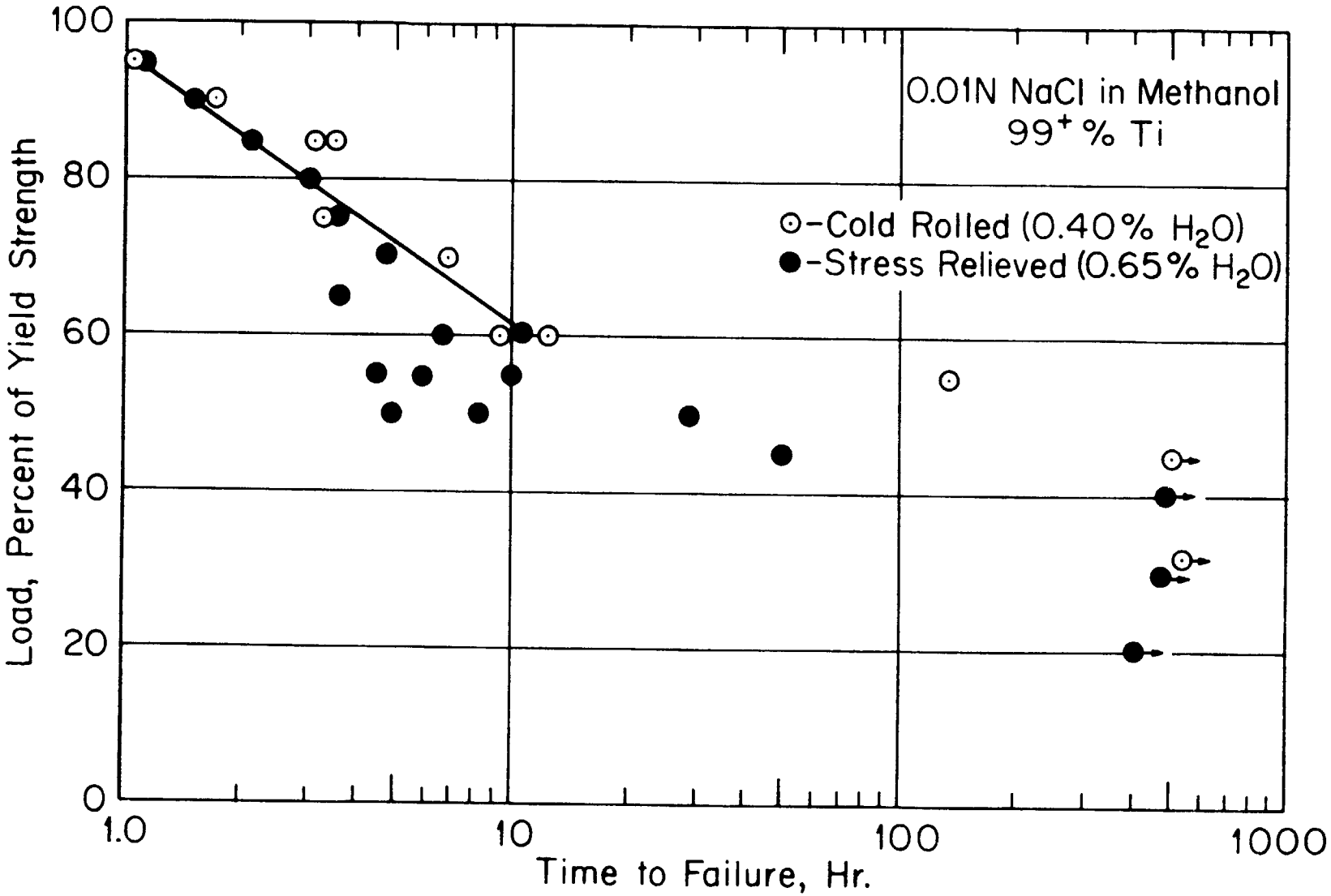

Figure 24 Variation of time to failure with applied load for 99^{+}% Ti with water added to the methanol for maximum susceptibility to stress corrosion.

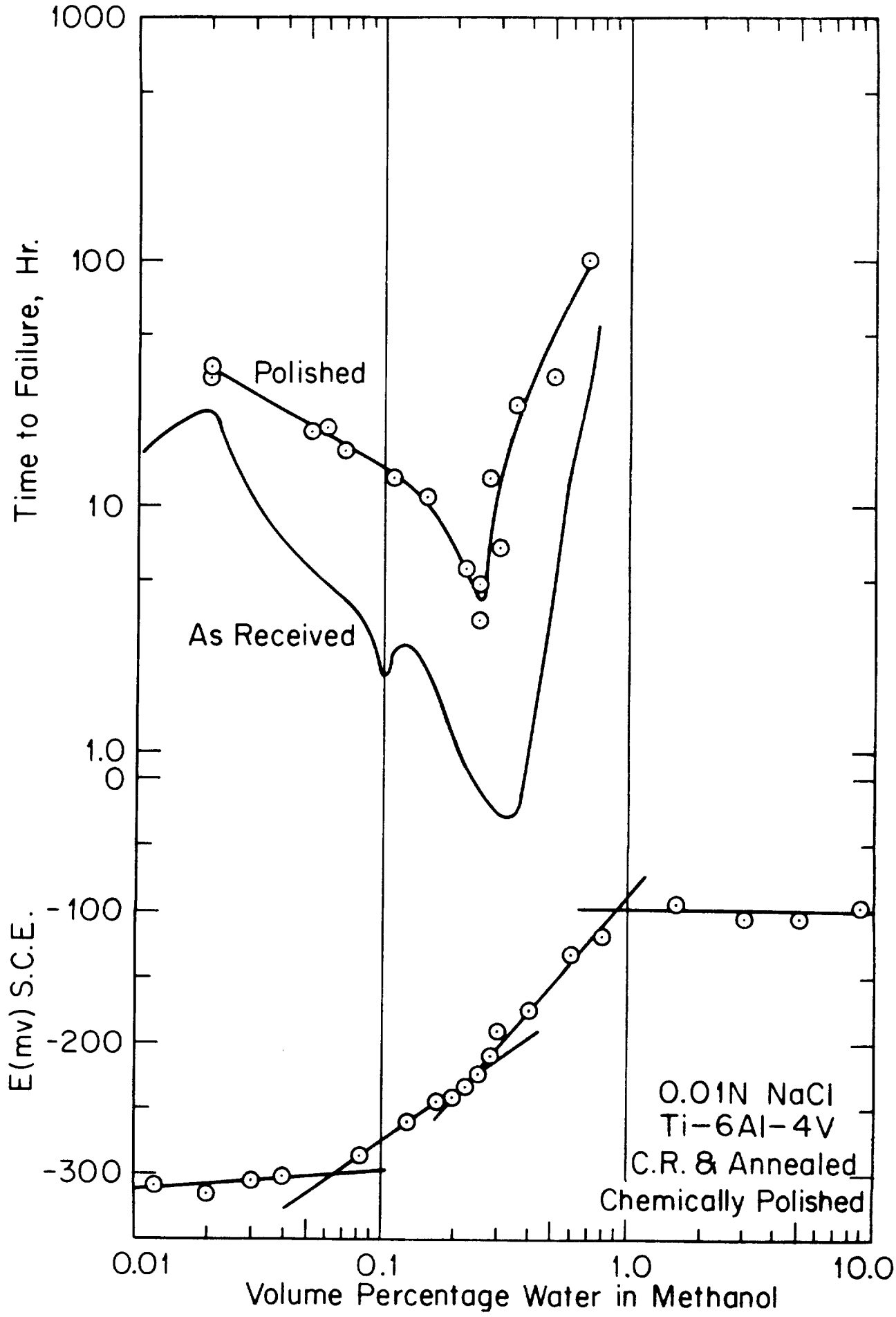

Figure 25 Comparison of time to failure with one-hour electrode potential value.

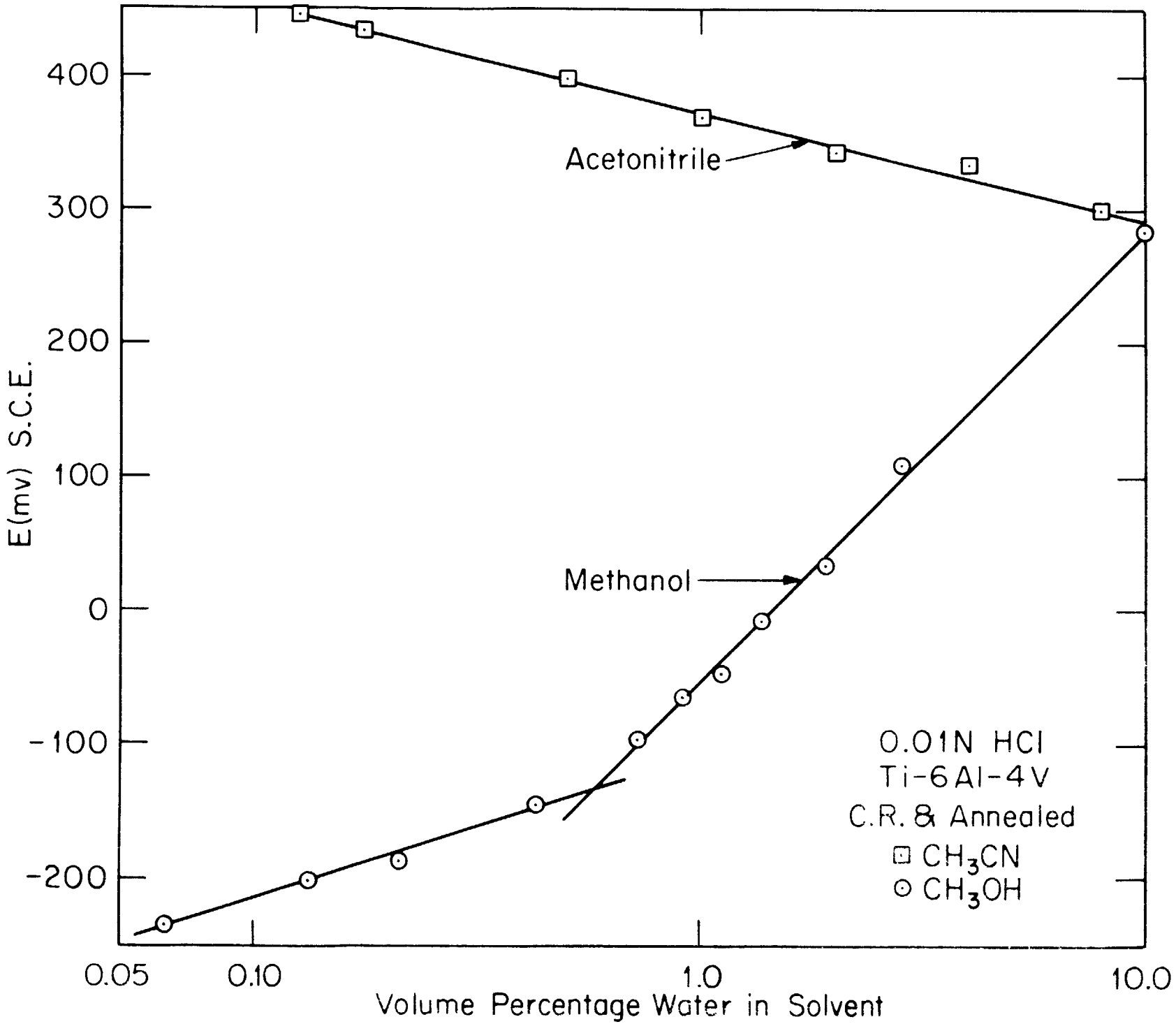

Figure 26 Comparison of one-hour electrode potential values for acetonitrile and methanol.

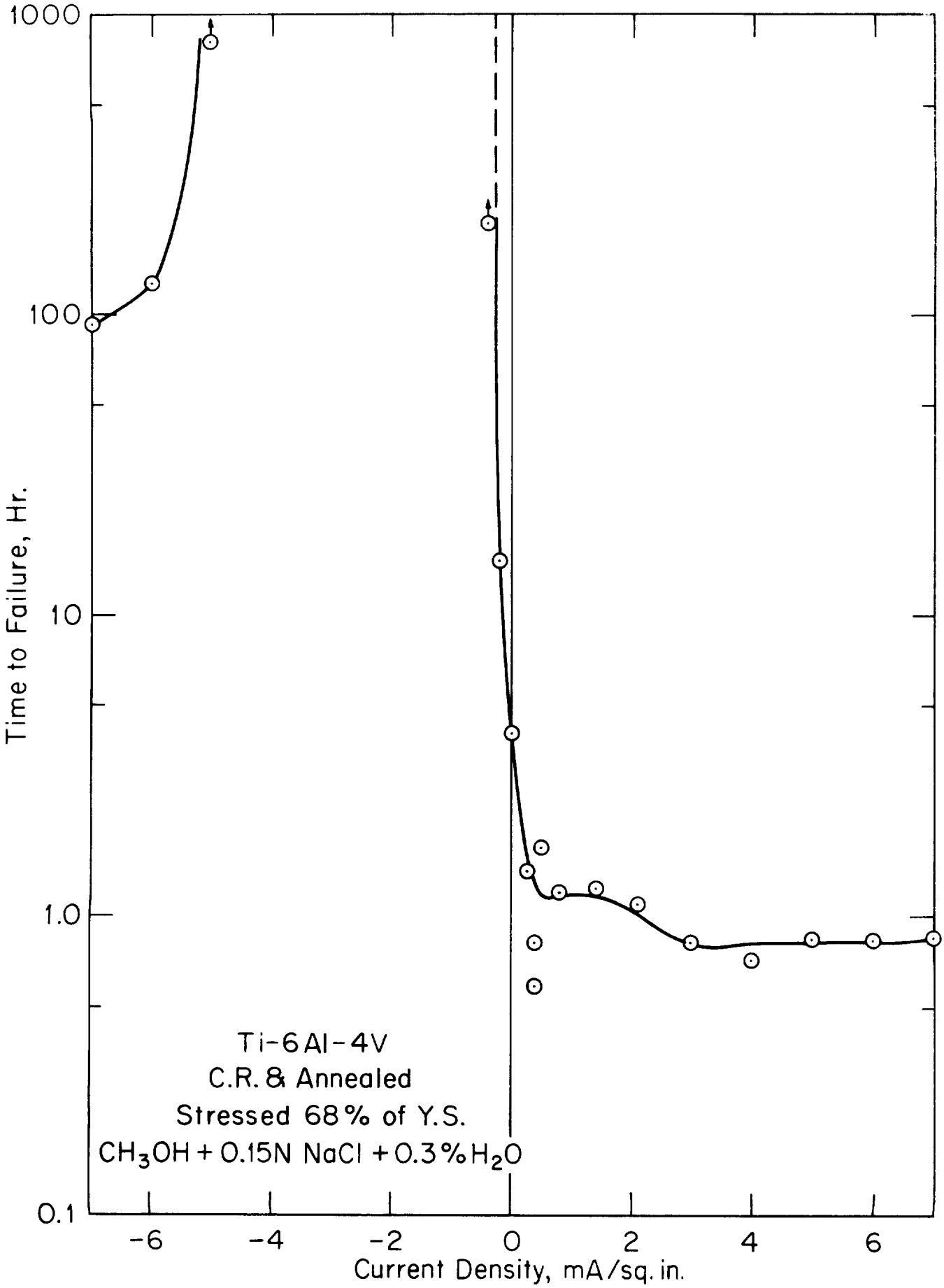

Figure 27 Effect of cathodic and anodic polarization on time to failure.

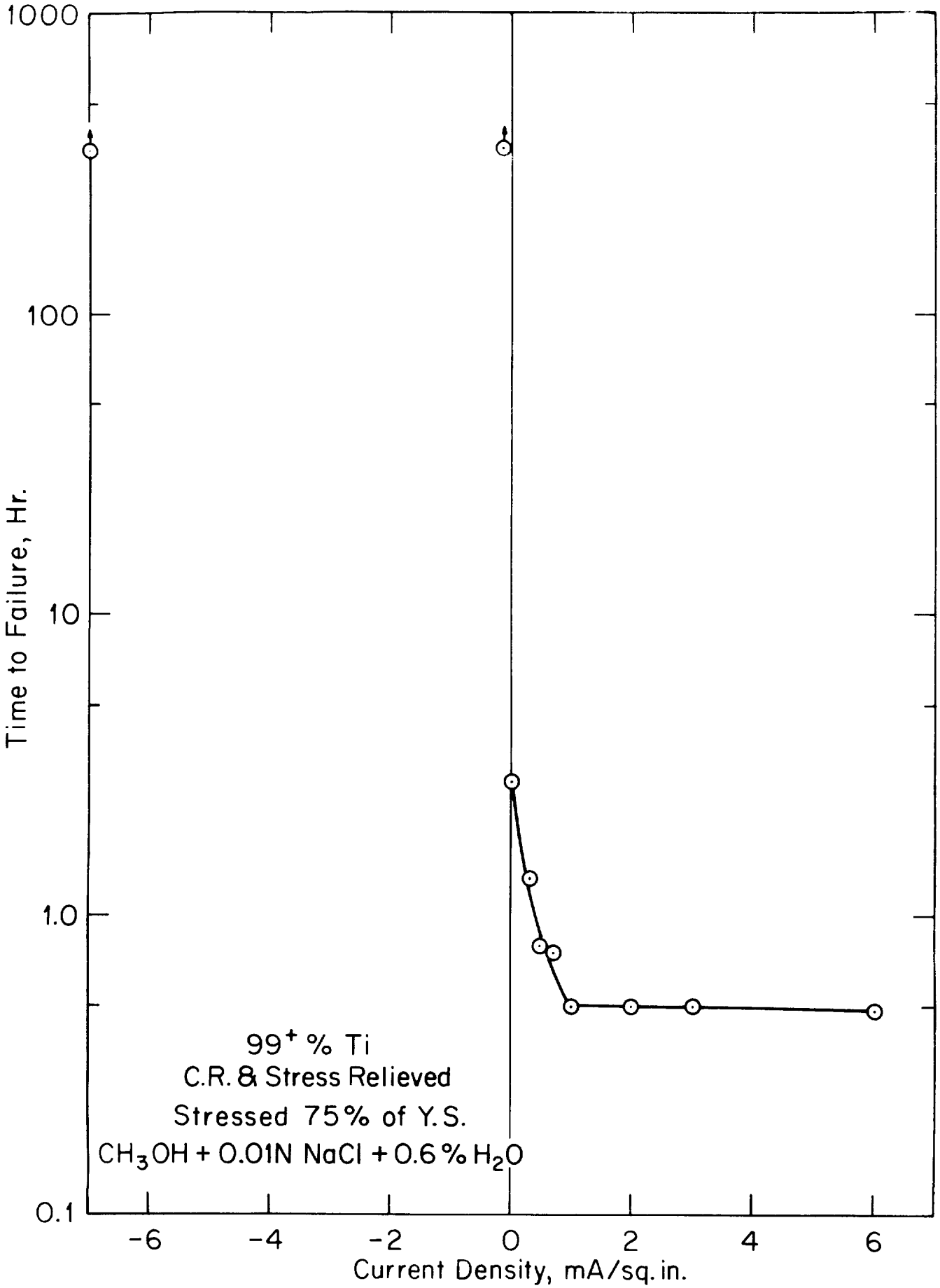

Figure 28 Effect of cathodic and anodic polarization on time to failure.

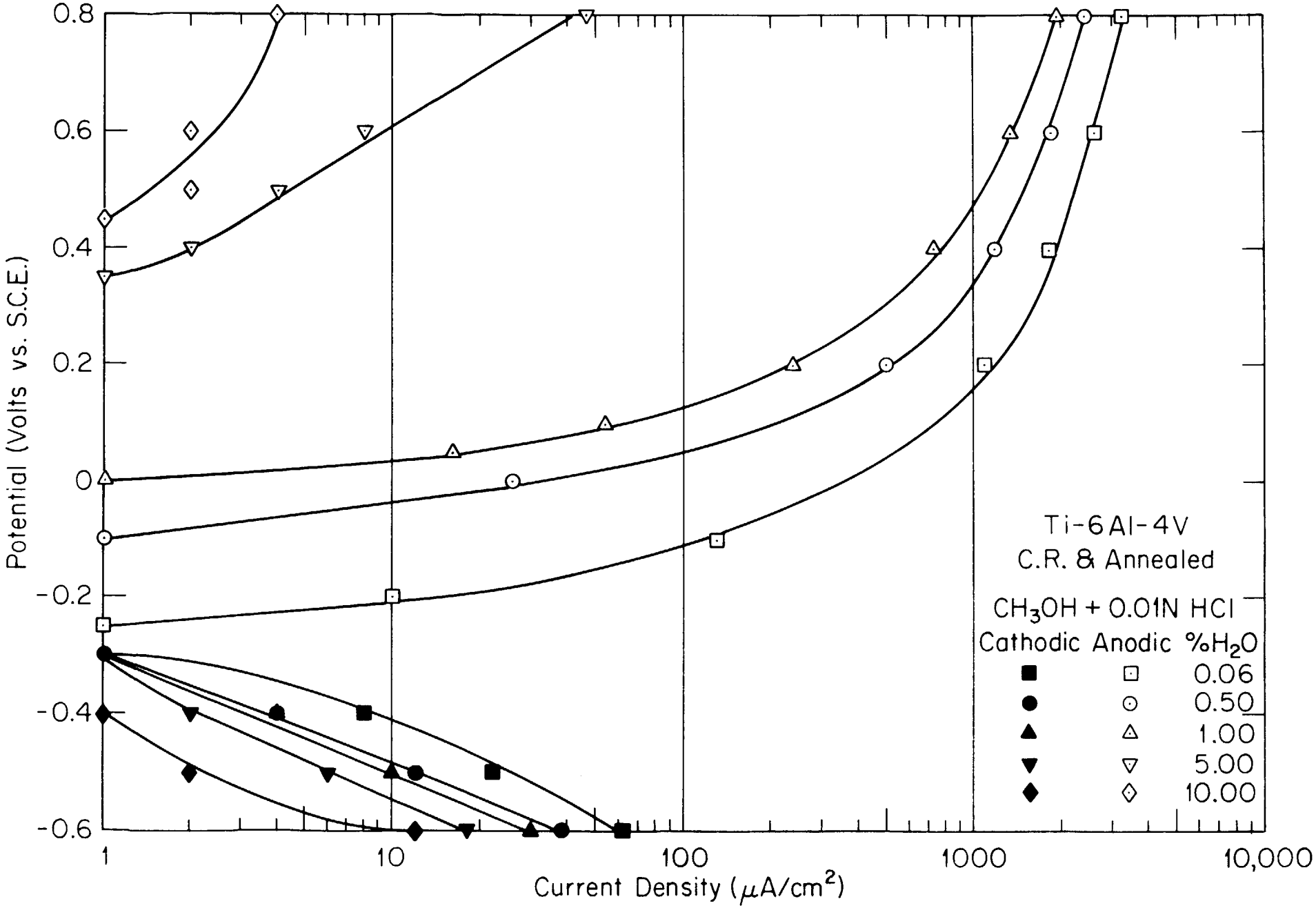

Figure 29 Cathodic and anodic polarization curves.

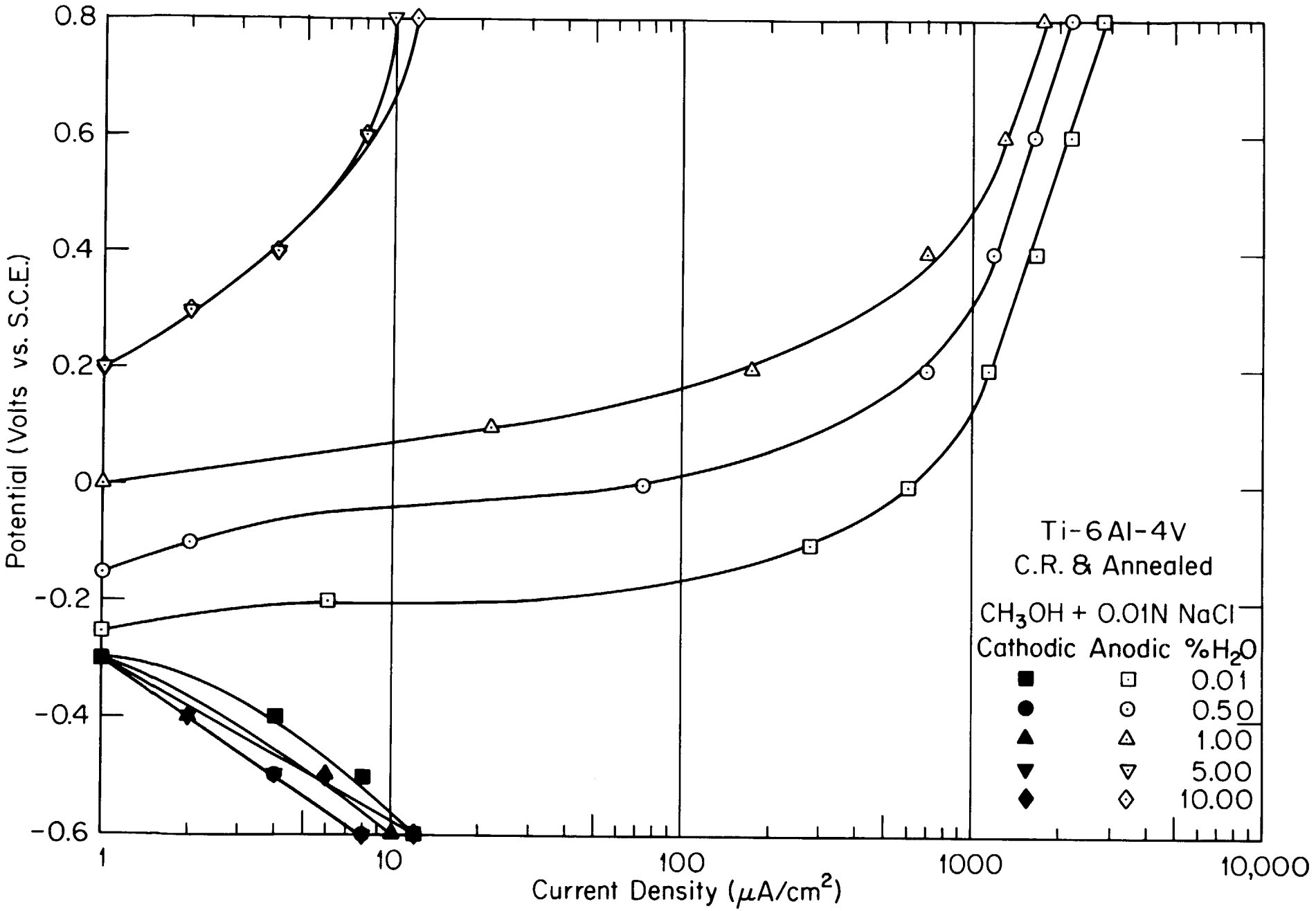

Figure 30 Cathodic and anodic polarization curves.

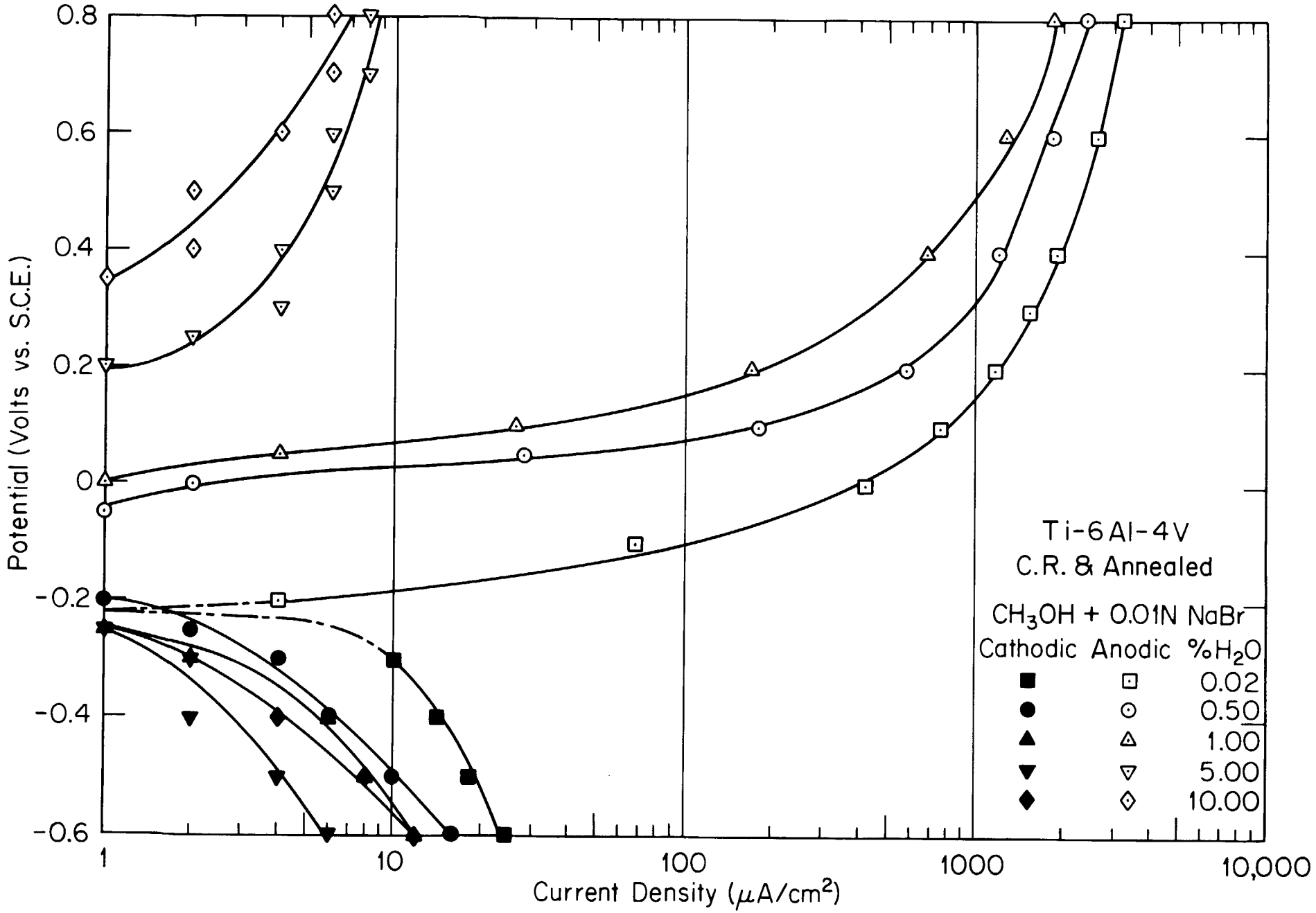

Figure 31 Cathodic and anodic polarization curves.

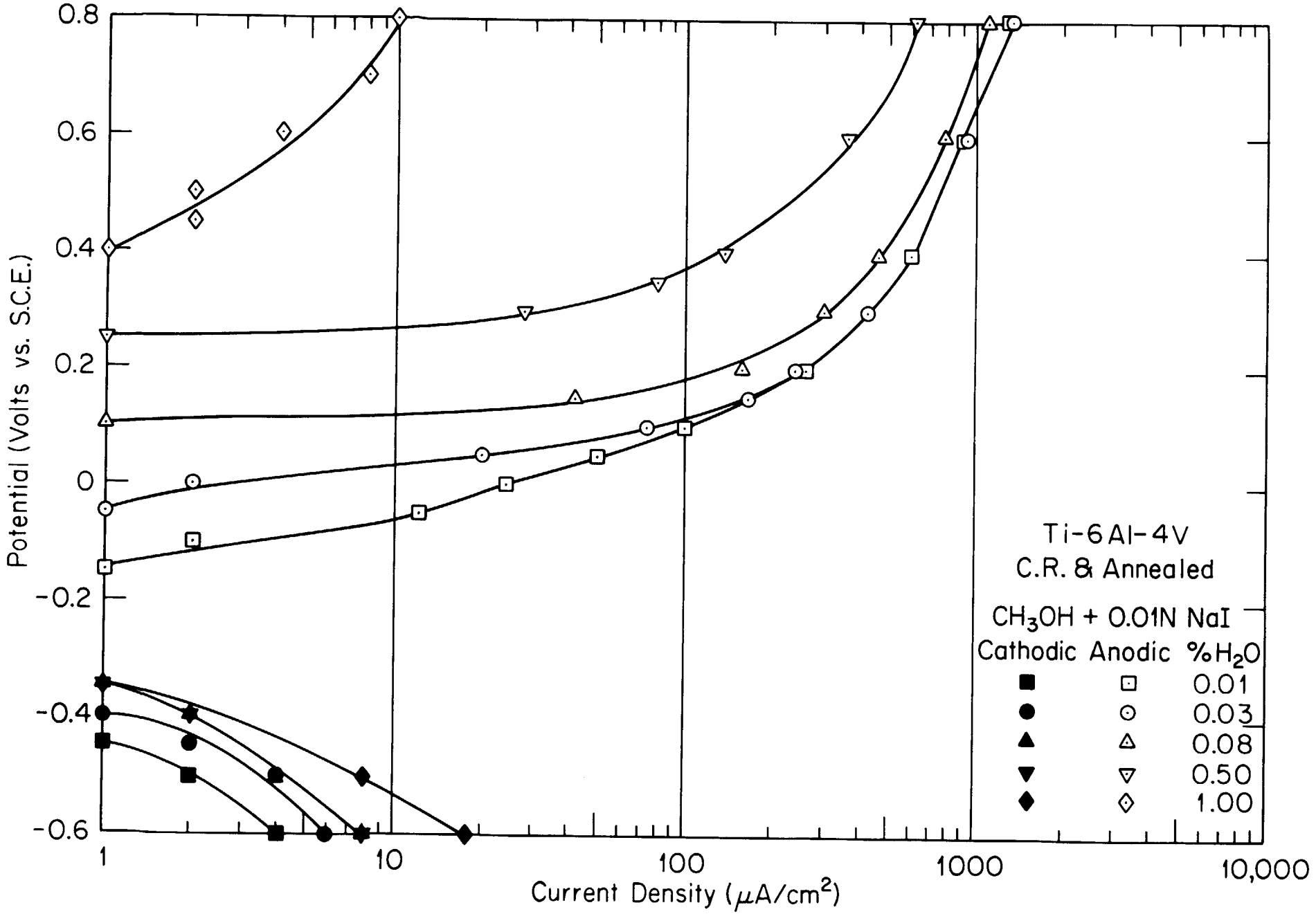

Figure 32 Cathodic and anodic polarization curves.

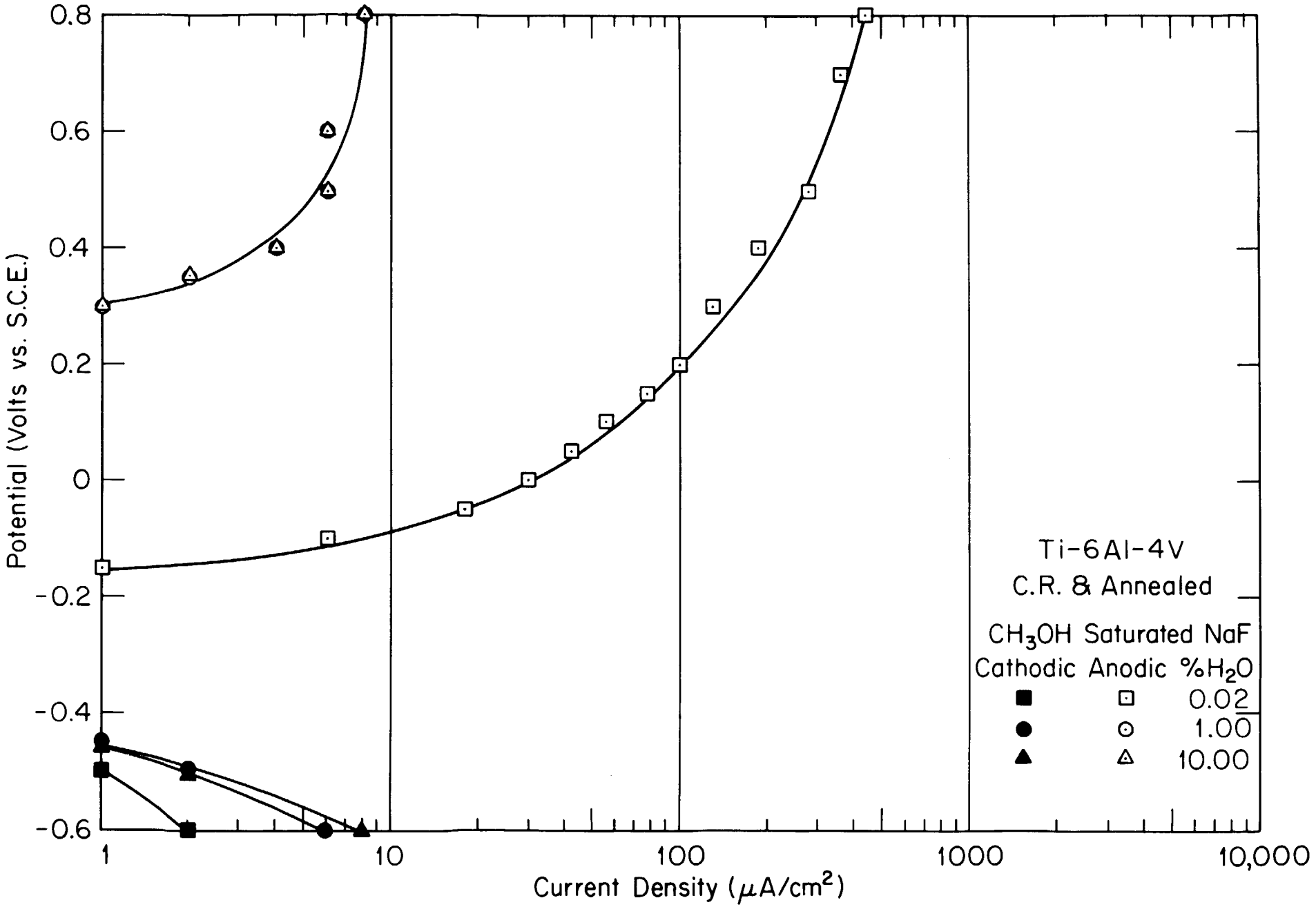

Figure 33 Cathodic and anodic polarization curves.

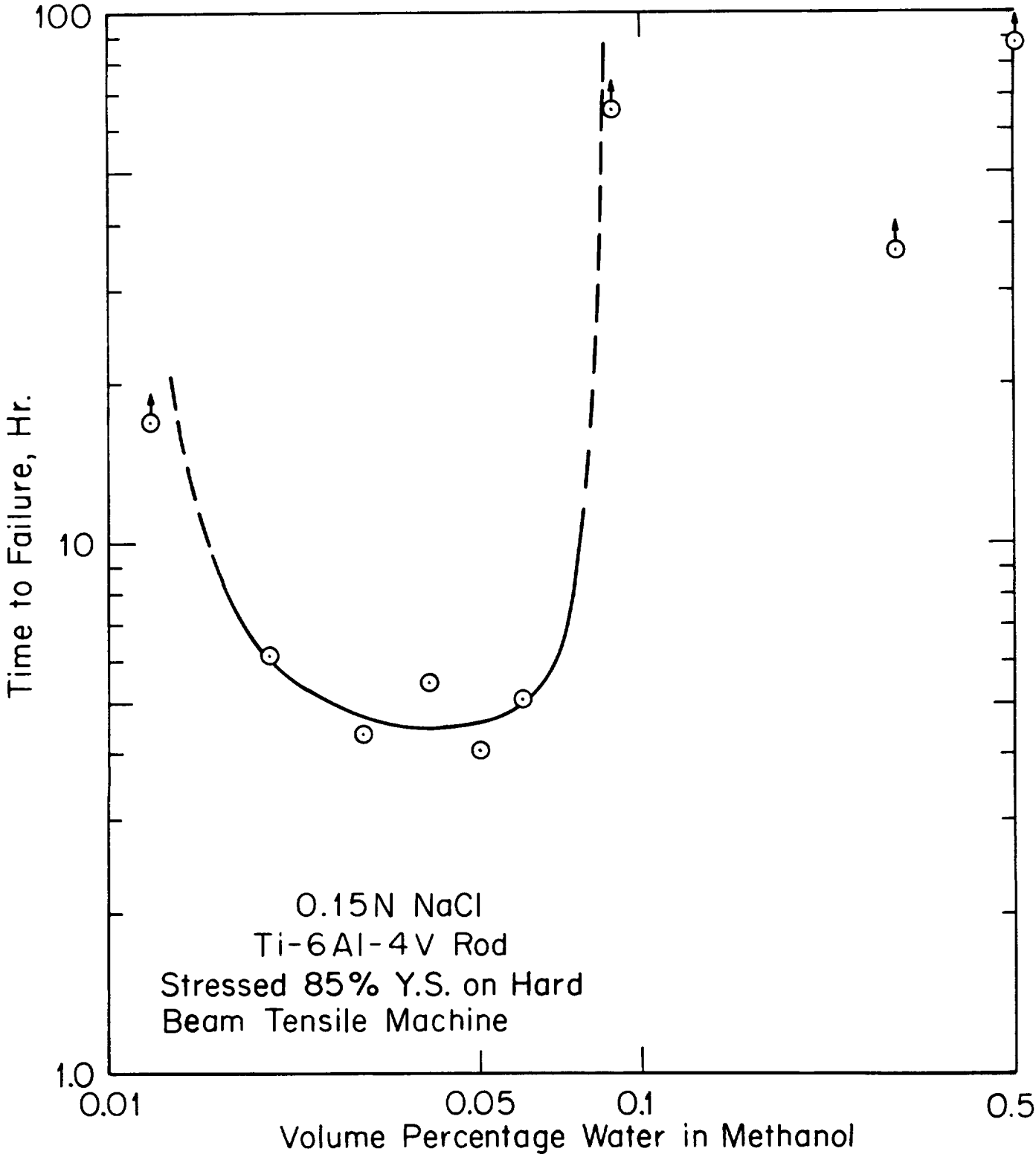

Figure 34 Time to failure curve for cylindrical specimen.

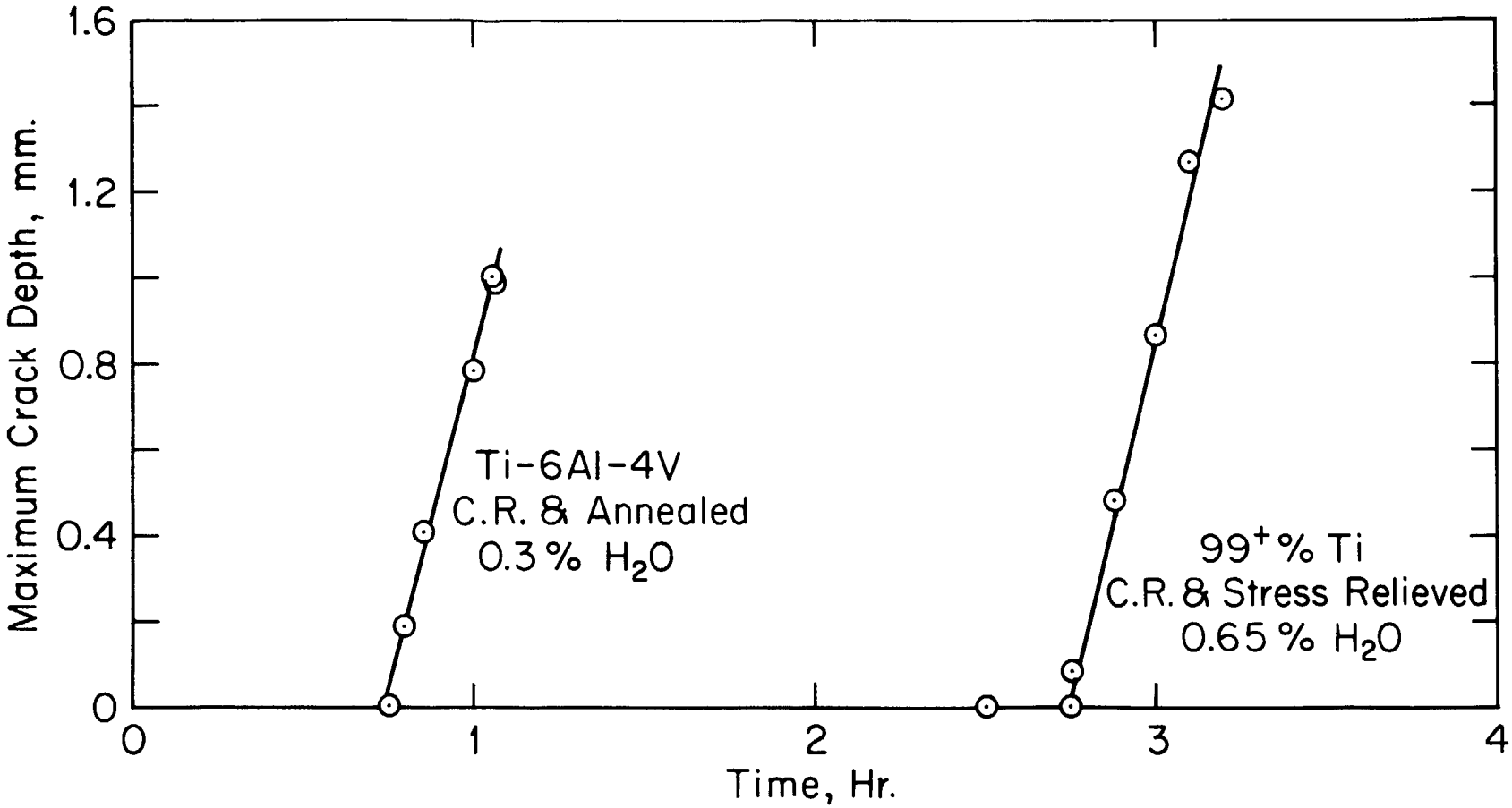

Figure 35 Curve of maximum crack depth vs. time for Ti-6Al-4V and 99^+% Ti foils in methanol with 0.01N NaCl solutions stressed at 75% of yield strength.